APL Photonics

PERSPECTIVE | NOVEMBER 13 2020

VO_2 nanophotonics

Sébastien Cueff ; Jimmy John; Zhen Zhang; Jorge Parra ; Jianing Sun; Régis Orobtchouk ; Shriram Ramanathan; Pablo Sanchis

APL Photonics 5, 110901 (2020)
https://doi.org/10.1063/5.0028093

VO_2 nanophotonics

Cite as: APL Photon. 5, 110901 (2020); doi: 10.1063/5.0028093
Submitted: 2 September 2020 • Accepted: 18 October 2020 •
Published Online: 13 November 2020

Sébastien Cueff,[1,a] Jimmy John,[1] Zhen Zhang,[2] Jorge Parra,[3] Jianing Sun,[4] Régis Orobtchouk,[1] Shriram Ramanathan,[2] and Pablo Sanchis[3]

AFFILIATIONS

[1]Université de Lyon, Institut des Nanotechnologies de Lyon (INL) UMR 5270 CNRS, École Centrale de Lyon, 36 avenue Guy de Collongue, 69134, Ecully, France
[2]School of Materials Engineering, Purdue University, West Lafayette, Indiana 47907, USA
[3]Nanophotonics Technology Center, Camino de Vera s/n, Universitat Politècnica de València, Valencia 46022, Spain
[4]J. A. Woollam Co., Inc., Lincoln, Nebraska 68508, USA

[a]**Author to whom correspondence should be addressed:** sebastien.cueff@ec-lyon.fr

ABSTRACT

The intriguing physics of vanadium dioxide (VO_2) makes it not only a fascinating object of study for fundamental research on solid-state physics but also an attractive means to actively modify the properties of integrated devices. In particular, the exceptionally large complex refractive index variation produced by the insulator-to-metal transition of this material opens up interesting opportunities to dynamically tune optical systems. This Perspective reviews some of the exciting work done on VO_2 for nanophotonics in the last decade and suggests promising directions to explore for this burgeoning field.

I. INTRODUCTION

Nanophotonics has enabled tremendous advances in the understanding of light–matter interaction and opened up new ways to control light at the nanoscale.[1–3] Through the arrangement of designed nanostructured materials, a myriad of possibilities has recently emerged for applications in datacom, quantum optics, displays, bio-sensing, or wavefront shaping. In particular, recent progress in dielectric metasurfaces made possible the design and fabrication of flat optics devices that hold promise to replace conventional bulk optics.[4,5] At optical frequencies ranging from the UV to the mid-infrared (MIR) regions, nanophotonic systems are patterned at the micro- and nano-scale, resulting in building blocks whose geometries and arrangement are definitively set after fabrication. Such low-dimensional devices are static, which makes the dynamic variation of their physical properties not exempt of challenges. Most (if not all) nanophotonic applications would strongly benefit from tunable and reconfigurable properties, and finding solutions to overcome such challenges is currently an intense field of research in which many different strategies are explored. A non-exhaustive list would include electro-mechanical systems, liquid crystals, thermal modulations, non-linear optics, and piezoelectric effects. More recently, phase-change materials (PCMs) have become a popular method of optical tunability without any moving parts. These materials are indeed very promising to enable dynamic modification to the physical properties of devices at the micro- and nanoscale. PCMs are a class of materials with unique physical properties: their structural arrangement can be controllably modified back and forth on a fast timescale using a thermal, electrical, or optical excitation.[6,7] For some of these materials, the crystallographic re-arrangement translates into a large refractive index modification ($\Delta n \geq 1$). Such a large and fast refractive index modulation is a long-sought effect for photonics: an enabling technology to control and tune in real-time the optical properties of devices at the nanoscale.

Among them, vanadium dioxide (VO_2) is a prototypical example of functional materials showing large modifications in their physical properties upon specific external excitation. The complex physics of VO_2—which we will briefly describe later in this Perspective —ignited discussions among researchers on whether this material should belong to the class of PCMs. Regardless of this debate, we feel that the term PCM is particularly well-suited to group together materials whose optical properties can be dynamically modified via a change in their atomic structure, a definition that works for both

the tunable chalcogenide materials (e.g., GST and GeTe) and oxides (VO_2).

The insulator-to-metal transition (IMT) partly governing the drastic physical changes in VO_2 was first discovered by Morin in 1959 during his investigations on the temperature dependence of electrical conductivity in several transition-metal oxides.[8] A few years later, another team of researchers from the same laboratory (Bell Labs) published a complete experimental dataset of the optical properties of VO_2 above and below the transition temperature, which were found largely tunable for both bulk crystals and thin films.[9,10]

Decades later, in the late 2000s, after years of intense fundamental research on this fascinating material, VO_2 started to be integrated in photonic devices, driven by the need to dynamically modify the response of optical metamaterials.[11–13] Since then, VO_2 thin films have been exploited in a plethora of devices, concepts, and systems in the field of nanophotonics. In this Perspective review, our motivation is therefore to summarize this decade of research exploiting the IMT of VO_2 to dynamically modulate nanophotonic devices and systems.

A few reviews on the physics and properties of VO_2 can already be found in the literature.[14–16] They are, in most cases, either dedicated to understanding the complex physics of this material or to review their multiple possible applications. The objective of the present Perspective is not to add another layer of extensive review of all research studies conducted on VO_2. Our goal here is to give an in-depth and specific look at the recent results obtained on VO_2 applied to nanophotonics in wavelength ranges from the UV to the mid-infrared. We will see that this topic alone has already garnered so much interest that a review paper appears to be necessary. From there, we want the reader to get an overall panorama of current research on the field and on future promising perspectives.

In Sec. II, we briefly describe the intriguing physics of VO_2 and explain the origin of the transition observed in this material. In Sec. III, we then describe in more detail the optical properties of VO_2 and give recommendations to study and analyze them. Section IV is dedicated to review recent works on VO_2 for integrated guided wave optics, and Sec. V is focused on VO_2-based metasurfaces for free-space photonics. In Sec. VI, we describe a few interesting directions to explore that we find particularly promising for future works on the field, namely, the electrical control, the absorption mitigation, the spatial addressability combined with the memory effect, and the ultrafast switching of VO_2.

II. THE PHYSICS OF VO_2

VO_2 is a particularly complex material with extremely rich physics that have been actively investigated in the past decades. It is a prototypical example of correlated oxides and Mott insulators. Describing the physics of Mott insulators is outside the scope of this Perspective paper, and we refer the readers to several excellent reviews on the topic.[17,18] However, the basic physics behind this phenomenon can be understood as follows. Band theory has proven to be a very powerful tool to predict and understand the physical properties of materials with known elements arranged in a specific crystallographic structure. This has helped classify materials in "boxes" according to their physical properties, linked to their band diagram. For example, insulators have their Fermi level in a bandgap, while metals have their Fermi level inside a partially filled band. The distribution of energy and carriers, as calculated through the energy band diagrams, therefore dictates the physics of the materials. However, for some materials, this band theory fails, at least partially. Indeed, the physical properties of some transition-metal oxides do not follow band theory. VO_2 is one of the most well-known examples of such materials: it has a partially filled d-electron band and, according to band theory, should therefore behave as a metal but surprisingly shows insulating properties at room temperature. This unexpected effect is due to the strong electron–electron Coulombic repulsion that exists in this material and is not taken into account in band theory. Such a correlation between electrons "freezes" them in their sites and prevents electrical conduction: this is the basic principle of Mott insulators and strongly correlated materials such as VO_2. The IMT is a natural consequence of this strong electron–electron correlation: an appropriate stimulus will break this equilibrium (e.g., heat, above 70 °C) and electrons will start to behave as free carriers, similarly as in a regular metal.

Simultaneous to this IMT behavior, VO_2 undergoes a structural change from a monoclinic phase M1 with space group of $P2_1/c$ at room temperature to a rutile phase with space group of $P4_2/mnm$ at temperatures above 70 °C.[8] Under strain[19] or doping with, e.g., Al or Cr,[20–22] another type of monoclinic phase M2 with space group of $C2/m$ and triclinic phase T with space group of $P1$ were stabilized. These monoclinic phases M1 and M2 and triclinic phases possess different patterns in V–V bond length and volume change with respect to the rutile phase. A thermodynamic phase diagram has been established experimentally by Park *et al.*, which illustrates the stability of these monoclinic phases in various strain-temperature windows.[19]

This crystallographic transition does not simplify the analysis and understanding of the overall physical properties. Peierls suggested that the structural change induces a lattice deformation, which modifies the periodic ionic potential in the material, resulting in a band structure change.[23] Consequently, we have at least two possible explanations as to what could be the driving force and the physical mechanism behind the transition of VO_2. On the one hand, we have the evidence of strong electron–electron correlation, suggesting a Mott–Hubbard scenario with strong Coulomb interaction between electrons, triggering the insulator–metal transition.[24] On the other hand, a structural transformation with strong dimerization, as predicted by Peierls, is also possible, wherein modification of the band structure is caused by the lattice distortion. Critical theoretical works in the last couple of decades by Eyert,[25,26] Biermann *et al.*,[27] He and Millis,[28] and van Veenendaal,[29] among others, have described the electronic structure as well as the magnetic ground state of vanadium dioxides.[14] Using first principles studies, Eyert reproduced the basic features of rutile and monoclinic phases with density functional theory and local-density approximations.[25] With hybrid functional corrections, better agreement with experiments such as bandgaps and antiferromagnetic ordering has been obtained.[26] Based on cluster dynamical mean field theory within density functionals, Biermann *et al.*[27] suggested that correlation assisted dynamical V–V singlet pairs play a critical role in the transition of VO_2. Recent theoretical studies on the transition and band structure suggested an intermediate theory combining both Peierls and Mott, described in terms of Mott-assisted Peierls transition.[30] This theory seems also consistent with the recent reports of

a photoinduced transient "metal-like" state of VO_2 that is produced without modifying the monoclinic phase, hence indicating a purely electronic transition.[31,32] The ultrafast THz phase diagram reported by Cocker *et al.*[33] shows that by increasing the incident laser fluence, the rutile phase can be nucleated and stabilized. Below 180 K, a transient metallic monoclinic state emerges prior to the nucleation of the rutile phase. This photoinduced ultrafast dynamics of VO_2 is consistent with the theoretical models proposed by He and Millis[28] and van Veenendaal[29] in critical fluency, coherent structural motion, and metastable M1 metal phases. The difficulty in experimentally untangling the structural and electronic aspects of this transition[34,35] due to the transient nature poses further challenges to this field. Further technique developments to probe local dynamics of phase evolution under external fields will be important as this class of materials becomes more widely studied and is implemented in device technologies.

Regardless of the intricate physical mechanisms governing the change of phase in VO_2, one of its main advantages is its multifunctional and multistimuli character. Indeed, the IMT of VO_2 can be induced using thermal heating (beyond $T_c \sim 70\,^{\circ}C$ at standard pressure), applied electric fields ($E = 10^5$ V cm^{-1}),[36,37] injected carrier densities ($n_e = 10^{18}$ cm^{-3}),[38] and optical[39,40] and terahertz pulses.[41] Conversely, this material and its IMT can then be used as an electrical switch, a thermal modulator, a thermochromic window, and an optical attenuator, to name just a few. For more details on all the possible applications of VO_2, we refer the readers to recent reviews.[14,16]

III. OPTICAL PROPERTIES OF VO_2 AND RECOMMENDED METHODS TO STUDY THEM

The optical properties of VO_2 thin films can be affected by a variety of factors, including deposition conditions, post-treatments, lattice matching to substrates, microstructures, and impurity concentrations. Understanding the optical behaviors of each specific sample at insulating and metallic phases and their optical evolution through the IMT process is therefore not only crucial for further utilization but will empower the optimization of VO_2 performance as a tunable medium in various optical and optoelectronic devices. Describing the various growth methods and related fabrication strategies is outside the scope of the present Perspective paper, and we redirect the interested readers to a recent review focused on that aspect.[15]

In this section, we describe the optical properties of VO_2 and their relation to the thin film's structure and pinpoint some of the difficulties in analyzing these complex and tunable optical properties.

A. How to break correlations between thickness and complex refractive index

Spectroscopic ellipsometry has been the standard method to investigate the optical properties of thin VO_2 films. Their refractive indices across the characteristic IMT evolution have been reported from ultra-violet to infrared frequency ranges.[42–45] The most pronounced changes occur at infrared wavelengths (Fig. 1), where the refractive index value strongly decreases [Fig. 1(a)], and there is simultaneously a large increase in the extinction coefficient [Fig. 1(b)]. Around the transition temperature and above, Drude losses associated with the metallic delocalized electrons take the place of Lorentzian absorptions in the imaginary dielectric function ε_2, and the permittivity ε_1 gradually goes to negative, indicating the transition from the insulating to metallic phase [see Fig. 1(c)]. VO_2 therefore presents broad absorptions even in its insulating phase. Such a lack of transparency is known to pose great challenges to optically determine the film thickness due to the commonly observed correlations between the thickness and the refractive index for absorbing materials. The simplest method to prevent these correlations is to measure the film's thickness via alternative methods such as profilometry, AFM, or x-ray diffraction, hence avoiding the need to let the thickness be a free fit parameter. However, these methods are not necessarily relevant for very thin films having a non-negligible surface roughness. Another common strategy to break such correlations is to simultaneously analyze ellipsometric data acquired from films with different thicknesses. Assuming that the set of films have identical dielectric functions,[46] the thickness was regarded as the sole cause in varying ellipsometric data, thus enabling the independent determination of the thickness and refractive index. The main concern associated with this multi-sample approach is the assumption validity when applied to thin VO_2 films. Many findings contradicted this assumption, reporting optical properties that depend on the thickness,[44,47] due to several factors such as surface roughness and vertical gradients in microstructures and in stoichiometry.

Another approach that we find particularly suited to break the correlations is through analyzing IMT dynamic data using a tunable optical model while maintaining a constant thickness to fit all states of VO_2.[43] This method focuses on the dominant effect on ellipsometric data originated from the evolution of dielectric functions during the phase transition process. By constraining the absorption resonance energies and linking oscillator parameters during the IMT, the correct thickness is expected to fit the large amount of spectroscopic data at various temperatures and different phases. The thickness can be confirmed through the uniqueness test—i.e., only one thickness value can fit all states of VO_2—and better sensitivity in the metallic phase was reported. Note that this method is only possible because the IMT of VO_2 does not modify the thin film thickness.

Other new methods could be found to break such correlations, but we emphasize that these correlations between thicknesses and complex refractive indices are very important, as one can easily (and unfortunately) overlook them during the analysis and thus obtain incorrect dispersion datasets.

B. Oscillator models and optical dispersion throughout the IMT

The imaginary dielectric functions, ε_2, of the insulating films deposited on silicon or silicon oxide substrates typically consist of two broad absorptions in the visible and near-infrared (NIR) spectrum, with center energy varying around 3.5 eV and 1 eV, respectively. As film grows thicker (>100 nm), a peak at ~2.1 eV becomes more distinguishable. For films on a sapphire substrate, the presence of this absorption peak has been unearthed at much lower thickness (~30 nm), which could be related to the improved film quality on sapphire even at the early stage of deposition. Each of these absorption peaks finds their physical roots in inter-band transitions between different orbitals (for more details, see, e.g., Ref. 14).

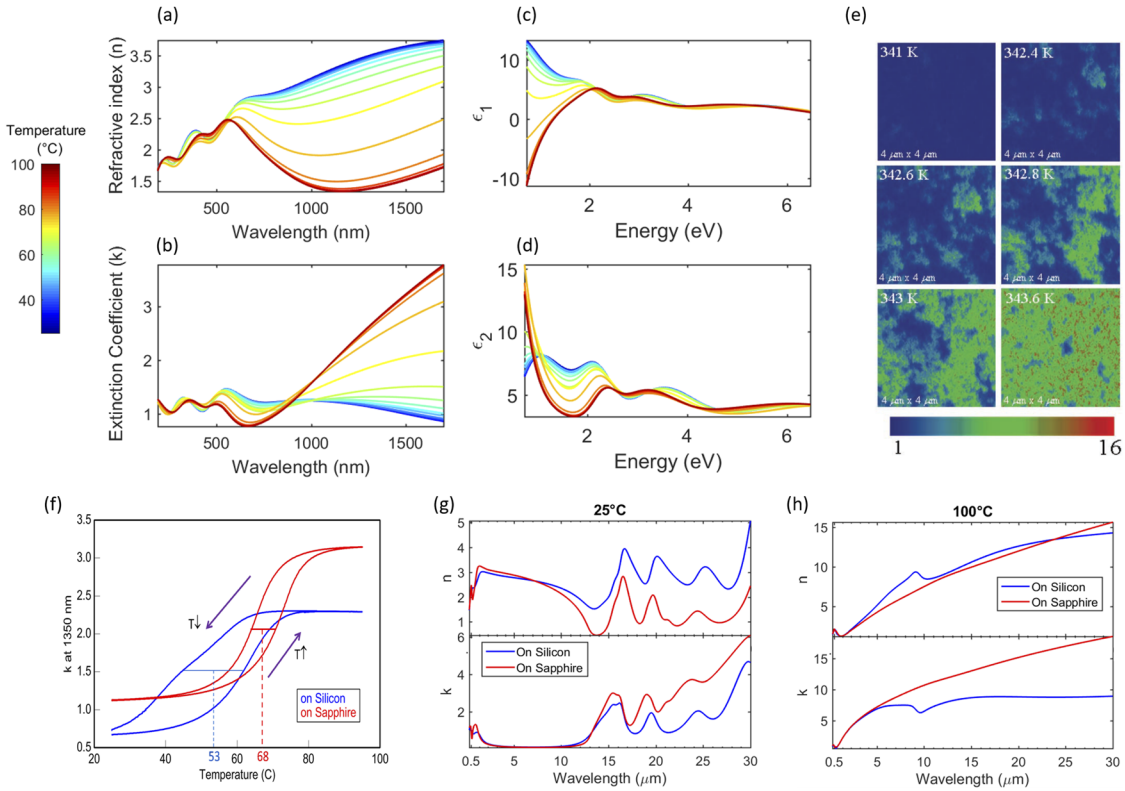

FIG. 1. Optical dispersion of the VO_2 thin film on sapphire, as extracted from temperature-controlled spectroscopic ellipsometry measurements: (a) refractive index *n*, (b) extinction coefficient *k*, (c) real part of permittivity ε_1, and (d) imaginary part of permittivity ε_2. (e) Scanning near-field infrared microscopy images showing the coexistence of insulating and metallic domains, with the progressive appearance of nanoscale metallic regions (represented in light blue, green, and red) during the IMT. Adapted with permission from Qazilbash *et al.*, Science **318**, 1750–1753 (2007).[48] Copyright 2007 AAAS. (f) Thermal hysteresis of the extinction coefficient (k) of the VO_2 film on Si and sapphire substrates at λ = 1350 nm, showing differences in optical properties and in phase transition behavior. Adapted with permission from J. Sun and G. K. Pribil, Appl. Surf. Sci. **421**, 819–823 (2017).[43] Copyright 2017 Elsevier. [(g) and (h)] Optical dispersion of VO_2 deposited on silicon and sapphire in the mid- and far-infrared regions. Adapted with permission from C. Wan *et al.*, Ann. Phys. **531**, 1900188 (2019).[44] Copyright 2019 Wiley.

Lorentz oscillators have been commonly applied to describe these absorptions.[10,43,49] The energies, amplitude, and broadening of these oscillators are adjusted across the IMT to accommodate optical changes induced by the phase transition. The Lorentz peak at ~1 eV red-shifts noticeably as temperature rises. It is eventually replaced by a Drude oscillator during the IMT to better represent the metallic absorptions. By monitoring these oscillator parameters through the thermal ramping process, Kakiuchida *et al.*[42] provided insights into band structural transition and bandgap changes through the IMT process.

During the IMT of VO_2, interesting regimes of intermediate phases occur, in which the medium becomes a combination of metallic and insulating regions, as shown via scanning near-field infrared microscopy [Fig. 1(e)].[48] Effective medium theory (EMT) has been applied to derive the optical properties of thin VO_2 films at these intermediate states when dynamic monitoring is not feasible. The method assumes the coexistence of insulating and metallic domains and approximates the refractive index based on the domain volume fractions at intermediate temperatures during the IMT process. The EMT method is potentially valuable in describing gradual transitions, such as VO_2 films on silicon substrates.[44] However, sharp optical changes in thin films with better quality or long-range order will greatly challenge the effectiveness of EMT models. The demand of drastic changes in oscillator parameters near the percolation transition could lead to failure in regression analysis or non-physical outcomes.

C. Influence of the substrate and microstructure on the optical properties and hysteresis

The film microstructure has been shown to strongly impact the optical properties of VO_2 films. Important information on the dynamic structural transformation of VO_2 can be obtained via various techniques such as x-ray diffraction, transmission electron microscopy, pump–probe electron diffraction, and Raman spectroscopy.[31,50–53] Using *in situ* real-time spectroscopic ellipsometry (RTSE), Motyka *et al.*[47] reported changing optical properties and structural variation during film growth and post-deposition treatments. A two-layer model revealed a more disordered/amorphous film with Lorentzian characteristics at an early stage of the deposition or at the film surface. As the film grows thicker, the bulk materials become better ordered with larger grain sizes and stronger

metallic conduction, leading to the potential shift of the bandgap to lower energy.

This structural and compositional dependence can also be found in the transition profile that can vary from abrupt to gradual and in the phase transition temperature that can be shifted depending on film quality, grain size, stoichiometry, degree of strain, and impurity concentrations.[43,45] Figure 1(f) shows the phase transition hysteresis loop and the transition temperatures optically determined from the reversible IMT thermal process on two different VO_2 samples. Thin films deposited on sapphire substrates present a sharp and narrow transition in comparison to the large hysteresis measured on films prepared on silicon.[43] These findings are consistent with resistivity measurement,[44,47] both resulting from better film quality on c-plane sapphire likely due to a smaller lattice mismatch at the film/substrate interface.

Wan *et al.*[44] studied the optical properties of VO_2 at both insulating and metallic phases from the visible to the far-infrared regions, as shown in Figs. 1(g) and 1(h). The complex refractive indices from 2 μm to 11 μm were reported to be less sensitive to the deposition process and film thickness. In that region, Drude losses dominate the metallic phase, while Lorentzian absorptions tapered down toward longer wavelengths at room temperature. Their measurements therefore indicate a spectral window (2 μm–11 μm) in which there are no, or negligible, microstructure- or substrate-dependence in the optical properties of VO_2 [see Figs. 1(g) and 1(h)]. On the other hand, they also noticed a couple of substrate-dependent features: in the metallic state, Lorentz absorption around ~10 μm was found to be absent for films on sapphire but present for films on silicon, likely due to other polymorphs of vanadium oxide. Moreover, strong vibrational resonances with distinctive substrate-dependence were observed between 17 μm and 25 μm at insulating states. Further investigation on the cause of these absorptions is necessary in tuning VO_2 films for infrared applications.

The crystalline structure of VO_2 theoretically present anisotropy. In most cases though, an isotropic optical model will sufficiently describe VO_2 thin films due to the following reasons. First, the films may consist of polycrystalline domains of different orientations, or different polymorphs of VO_x, resulting in isotropic behaviors on a macroscopic scale. This is typically what happens when VO_2 is deposited on Si or SiO_2.[15,54,55] Second, the optical measurement is generally less sensitive to the out-of-plane refractive index for a very thin absorbing film. Finally, as we have seen before, in some cases, correlations between the thickness and the refractive index for thin absorbing films add uncertainties to the accuracy and reliability of anisotropic analysis. More confidence in identifying anisotropy would be expected in thicker films with better crystallinity and stoichiometry control.

As we have seen in this part, the optical properties of VO_2 as well as the transition behavior are affected by a number of factors mainly linked to the substrate, thickness, and microstructure of the VO_2 thin film. It is therefore crucial to carefully analyze the optical properties of each VO_2 sample to adapt future devices' design to its specificity.

IV. VO_2 FOR GUIDED INTEGRATED PHOTONICS

Photonic integrated circuits (PICs) allow us to exploit the benefits of light for communication and data processing at the micro- and nano-scale. To this end, silicon has become the mainstream technology for novel developments in a wide variety of applications (datacom, telecom, sensing, high-performance computing, etc.).[56–58] However, silicon is not a particularly well-suited material for enabling active functionalities due to its intrinsic properties. In particular, the control of the optical phase and/or optical amplitude based on the plasma dispersion effect usually yields trade-offs among speed of operation, energy consumption, insertion losses, or footprint.[56] Silicon active devices with switching speeds in the picosecond timescale are possible. However, active lengths in the millimeter range are typically required for enabling large extinction ratios. More compact devices can be achieved by using resonant structures but at the expense of significantly narrowing the optical operation bandwidth. In this context, the hybrid integration of silicon with CMOS-compatible materials featuring unique properties has opened a path to achieve ultra-compact, broadband, and highly efficient guided photonic devices.[59] Such types of devices are desired to develop advanced PICs with complex functionalities and large-scale integration. As has been mentioned, VO_2 stands out for the ultra-large change in its complex refractive index between the insulating and metallic states. This feature enables hybrid tunable VO_2 waveguides with lengths down to hundreds of nanometers. Moreover, these kinds of waveguides are broadband since the changes in the VO_2 refractive index span a spectral range from the visible to the mid-infrared wavelength regions. The scheme of a commonly reported hybrid VO_2/Si waveguide is depicted in Fig. 2. The latter comprises a silicon waveguide with a patch of VO_2 atop. By triggering the IMT of VO_2 with an external excitation (heat, electric field, or light), the guided mode could experience a change in both optical phase and amplitude.

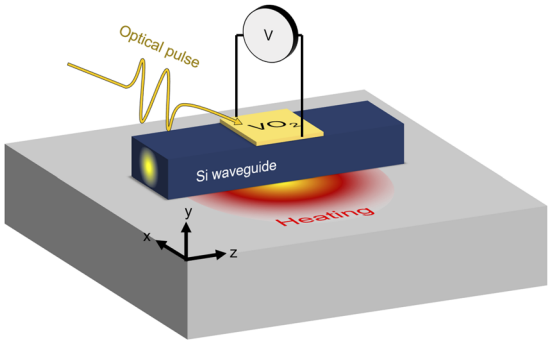

FIG. 2. Scheme of a hybrid VO_2/Si waveguide and different external excitations to control its properties.

In the following, we describe recently reported results, organized in three different parts, according to the methods used to trigger the IMT of VO_2.

A. Thermally modulated VO_2/Si waveguides

Several hybrid VO_2/Si waveguide devices, intended to function as amplitude modulators, have been proposed and demonstrated by thermally triggering the IMT.[54,60–67] To this end, the temperature of the chip can be controlled using a Peltier device or local heat into the VO_2 patch can be applied using Joule heating with metallic microheaters. One of the first hybrid VO_2/Si devices [Fig. 3(a)]

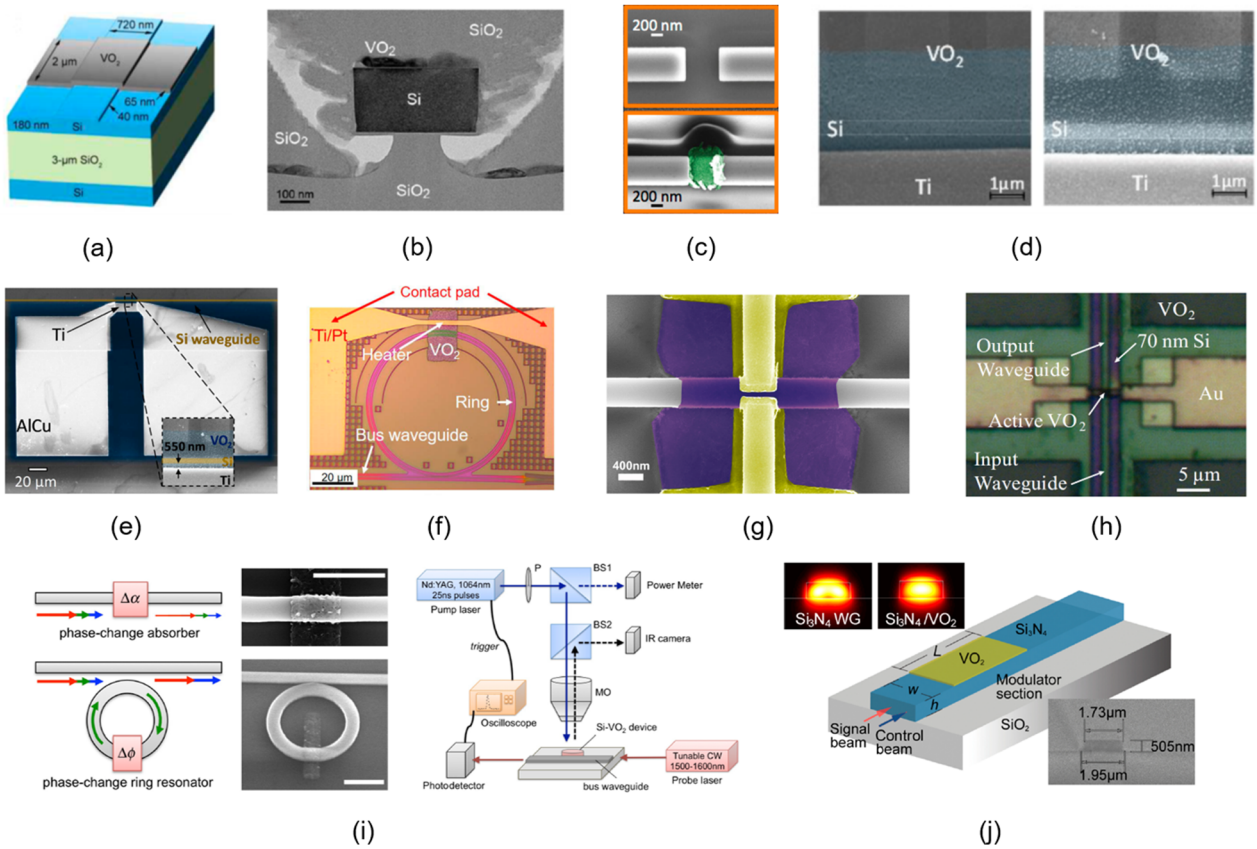

FIG. 3. Hybrid VO_2/Si waveguide devices. The first and most of the proposed devices have been based on thermally triggering the VO_2 phase transition with switching times in the microsecond range. (a) The most common hybrid waveguides are developed by depositing VO_2 on top of (a) rib [adapted with permission from R. M. Briggs *et al.*, Opt. Express **18**, 11192–11201 (2010).[54] Copyright 2010 The Optical Society] or (b) strip silicon waveguides [adapted with permission from K. Shibuya *et al.*, Opt. Express **27**, 4147–4156 (2019).[60] Copyright 2019 The Optical Society]. (c) Shorter devices have been achieved by embedding VO_2 within the silicon waveguide [adapted with permission from K. J. Miller *et al.*, Opt. Express **25**, 26527–26536 (2017).[62] Copyright 2017 The Optical Society]. (d) Enhanced optical switching performance has also been demonstrated by engineering the morphology of the VO_2 layer [adapted with permission from I. Olivares *et al.*, Opt. Express **26**, 12387–12395 (2018).[63] Copyright 2018 The Optical Society]. In addition, novel applications have also arisen such as (e) polarizers [adapted with permission from L. D. Sánchez *et al.*, Opt. Lett. **43**, 3650–3653 (2018).[64] Copyright 2018 The Optical Society] and (f) switches based on add-drop ring resonators [adapted with permission from V. Jeyaselvan *et al.*, OSA Continuum **3**, 132–142 (2020).[66] Copyright 2020 The Optical Society]. Electrically controlled devices have been investigated for enabling faster switching times. In this case, an electric field is applied between two separated metallic contacts on top of the hybrid VO_2/Si waveguide as shown in (g) [adapted with permission from P. Markov *et al.*, ACS Photonics **2**, 1175–1182 (2015).[68] Copyright 2015 American Chemical Society] and (h) [adapted with permission from A. Joushaghani *et al.*, Opt. Express **23**, 3657–3668 (2015).[69] Copyright 2015 The Optical Society]. All-optical switching schemes could also be a promising route toward ultra-fast speed. (i) Most of the works have been based on pumping VO_2 with out-of-plane approaches [adapted with permission from J. D. Ryckman *et al.*, Opt. Express **21**, 10753–10763 (2013).[55] Copyright 2013 The Optical Society; and J. D. Ryckman *et al.*, Opt. Express **20**, 13215–13225 (2012).[76] Copyright 2012 The Optical Society]. (j) Recently, all-optical switching using an in-plane approach has also been demonstrated in a hybrid SiN waveguide [adapted with permission from H. M. K. Wong *et al.*, ACS Photonics **6**, 2734–2740 (2019).[80] Copyright 2019 American Chemical Society]. However, the timescale of the device was not reported. The feasibility of ultra-fast timescale modulation still remains an open question.

was demonstrated by Briggs *et al.*[54] They showed the capabilities of VO_2 for optical switching at telecom wavelengths with an active length of only 2 μm but with a moderate extinction ratio of 6.5 dB and insertion losses of around 2 dB. For a given polarization of the guided optical mode, there is always a trade-off between the extinction ratio and the insertion losses, and most groups try to enhance the former and reduce the latter by engineering the hybrid VO_2/Si waveguide. Extinction ratios of 16 dB and insertion losses of 3.8 dB have been demonstrated with an optimized 3-μm-long hybrid VO_2/Si waveguide [Fig. 3(b)].[60] Ultra-short hybrid VO_2/Si waveguides with a length of only 500 nm have also been demonstrated by embedding VO_2 within the waveguide instead of placing it on top [Fig. 3(c)].[62] In this configuration, extinction ratios with almost 10 dB but relatively high insertion losses of around 6.5 dB have been reported. The optical switching performance can be further improved by engineering the morphology of the VO_2 layer [Fig. 3(d)]. In such a way, insertion losses below 1 dB and extinction ratios above 20 dB with switching times in the microsecond range were demonstrated for a 20-μm-long hybrid VO_2/Si waveguide.[63] On the other hand, the integration of VO_2 on a silicon waveguide

could also open alternative applications such as tunable polarizers. Sánchez *et al.* demonstrated a 20-μm-long transverse-electric (TE) pass polarizer exploiting the polarization dependence loss of the hybrid waveguide [Fig. 3(e)].[64] They showed a rejection of 19 dB for the transverse-magnetic (TM) polarization in the active state together with switching times of few microseconds for a wavelength range between 1540 nm and 1570 nm. The integration of hybrid VO_2/Si waveguides in add-drop ring resonators could also enable 2 × 2 optical switches.[61] Recent experimental results have shown an extinction ratio up to 25 dB with an insertion loss of 1.4 dB by placing a 19-μm-long VO_2/Si waveguide in a ring resonator [Fig. 3(f)].[66]

B. Electrically controlled VO_2/Si waveguides

The control of the VO_2 phase transition in a hybrid waveguide has also been demonstrated by applying an electric field between two separated metallic contacts, as shown in Figs. 3(g) and 3(h). Such a scheme is more interesting for future integrated applications and should enable faster switching times compared to the purely thermal heating counterpart as the applied heat can be localized and confined only to the VO_2 patch on the chip. Markov *et al.* used this approach to investigate the electro-optical switching dynamics in an ultra-short VO_2/Si hybrid waveguide [Fig. 3(g)].[68] They showed switching times of less than 2 ns for the IMT. The relaxation time to fall back to the insulating state involved a thermal dissipation process making the recovery slower. Nonetheless, by limiting the current to reduce Joule heating, they predicted switching time of the relaxation down to 3 ns but at the expense of a lower extinction ratio. Joushaghani *et al.* demonstrated a similar electro-optic VO_2/Si switch [Fig. 3(h)].[69] They achieved a high extinction ratio of 12 dB in a 1-μm-long device with insertion losses of 5 dB. Moreover, by biasing VO_2 near the onset of the IMT, they tested the capabilities of the device as a photodetector and achieved a responsivity in excess of 10 A/W with optical powers lower than 1 μW. Several proposals have also been made for developing hybrid plasmonic modulators.[70–74] However, the experimental demonstration of such devices is still lacking. On the other hand, the overall power consumption highly depends on the VO_2 patch size and the external resistance required to limit the maximum current flowing in the metallic state and avoid damaging the electrical contacts.[75] Thus, the only reasonable solution to reduce the power consumption of electrically controlled devices with respect to thermal heating approaches is to design very short hybrid waveguides, what could restrict the maximum achievable extinction ratio.

C. Optically switched VO_2/Si waveguides

Finally, all-optical switching schemes to control the state of hybrid VO_2/Si waveguides could be the most promising approach. Notably, the switching timescale of the IMT, triggered by optical excitation, has been demonstrated down to the femtosecond and would allow ultra-fast speed with a seamless integration in PICs.[39,55,76–80] However, such a type of ultra-fast device has not been demonstrated yet. Ryckman *et al.* demonstrated the first all-optical hybrid VO_2/Si device.[76] They integrated the hybrid VO_2/Si waveguide in a small ring resonator and induced the IMT of VO_2 by pumping the patch out-of-plane with a pulsed laser in the visible. No switching times were reported, and the optical switching of VO_2 was attributed to be photothermal. Afterward, the same authors investigated the timescale of such devices [Fig. 3(i)].[55] In this case, they used a pulsed laser of a few nanoseconds to excite the IMT of VO_2. On the one hand, a fluence dependence in the completion of the IMT was observed. For this device, pump fluences above 12.7 pJ/μm^2 drove VO_2 to its metallic state. On the other hand, the measured IMT timescale was found similar to the pump-pulse width (~25 ns) with a minimum influence of the fluence. However, the switching time from the metallic to insulating phase (relaxation time) showed a high dependence with the fluence and the VO_2 patch size. By increasing the pump fluence above the threshold up to ~70 pJ/μm^2 and enlarging the VO_2 patch from 500 nm to 1 μm, the relaxation time increased from ~30 ns to ~3 μs. Thus, the relaxation dynamics were found to depend on the thermal diffusion of the monoclinic phase. Haglund *et al.* investigated the timescale of hybrid VO_2/Si waveguides [Fig. 3(c)] by illuminating out-of-plane the device with a femtosecond laser acting as a pump and using an in-plane probe laser to record any change in VO_2.[79] For this case, a 900-nm-long VO_2 patch reportedly showed switching speeds lower than 2 ps for fluences between 50 pJ/μm^2 and 100 pJ/μm^2. More recently, sub-ps switching times have also been demonstrated by optimizing the fluences and reducing the volume of VO_2 in the hybrid waveguide.[81]

While these are promising results, the out-of-plane excitation is not the best approach for integration in PICs, and future all-optical schemes with both the pump and the probe guided within the waveguide would be more desirable. All-optical switching with hybrid waveguides using an in-plane approach has been recently demonstrated.[80] In this case, SiN instead of Si was used for the hybrid waveguide to handle the pump between 700 nm and 1000 nm and the probe at 1550 nm [Fig. 3(j)]. An extinction ratio of 10 dB was achieved for a 5-μm-long hybrid waveguide with a switching energy as low as 6.4 pJ. However, the timescale was not reported. Parra *et al.* have recently addressed this question using a similar in-plane pump–probe technique in the telecom wavelength region with a hybrid VO_2/Si waveguide.[82] Their temporal results suggest a thermal dynamics in which the phase change of VO_2 is thermally triggered and therefore limited to the nano/microsecond range.

In view of this recent work, a remaining important challenge is to find ways to reach the femtosecond timescale of the IMT in integrated devices. Promising directions could be to precisely adjust the excitation source to only trigger the electronic IMT of VO_2 without introducing parasitic heat generation.[83–85] In addition, engineering the thermal environment of devices to efficiently dissipate heat would also greatly help minimizing the relaxation time of the IMT.

V. VO_2 METASURFACES AND METAMATERIALS FOR FREE-SPACE NANOPHOTONICS

Recent years have seen the emergence of optical metasurfaces.[4,5] In these devices, an abrupt phase/amplitude shift is printed on a surface through engineered nano-elements. By spatially arranging such meta-atoms on a substrate, one can design metasurfaces tailored for specific optical functionalities such as lenses, polarizers, retroreflectors, holograms, and perfect absorbers, among many others.[4,86–88] Some of these flat optics devices already surpass the

performances of conventional diffractive optics components. As this field is becoming mature with conventional "passive" materials, researchers are now actively seeking means to dynamically modify the properties of these nano-elements to demonstrate actively reconfigurable metasurfaces, what may revolutionize the field of integrated optics. We review in the following different approaches and concepts that exploit VO_2 to dynamically tune the free-space optical response of flat optics devices.

A. Tunable metasurfaces based on un-patterned thin films

A thin-film material with adjustable complex permittivity can be considered as the simplest form of a metasurface, especially if it presents spatial variations of permittivity. As described in Sec. III, across the transition of VO_2, intermediate states are produced, in which metallic and insulating phases coexist at the nanoscale. These different mixed states can be regarded as naturally disordered metamaterials with tunable optical properties, and in the following, we analyze the different features of these appealing states.

Perfect absorption was achieved by Kats *et al.* in a system where a thin layer of VO_2 (~180 nm) was grown on a sapphire substrate [Fig. 4(a)].[89] At temperatures close to the IMT [Fig. 4(b), ~343 K], the absorption losses equal the radiative losses and the so-called critical coupling conditions are reached, producing an absorption of 99.75% at a wavelength of $\lambda = 11.6\ \mu$m. Given that this near-perfect absorption is dynamically tunable, over the transition temperature range, the reflectivity at $\lambda = 11.6\ \mu$m can be largely modulated from 80% to 0.25%. Similarly, Butakov *et al.* reported broadband tunable reflection and transmission in a tri-layer system ($Ge/VO_2/Al_2O_3$) in the mid-infrared and demonstrated electrical tuning of such a system.[90] Furthermore, Rensberg *et al.* reported that the suppression of reflection can be engineered by depositing an ultrathin layer of VO_2 on epsilon-near-zero substrates such as aluminum-doped zinc oxide (AZO), SiO_2, and ZnO [Figs. 4(e)–4(g)], and tuned by temperature.[91] A minimum of reflectance is found close to the plasma resonance of AZO [Fig. 4(e)] and the reststrahlen band of SiO_2, while the local minimum is absent on ZnO. Conversely, as stated by Kirchhoff's law, the absorption is closely related to the thermal emission, implying that a good absorber should also be a good thermal emitter. As shown in Figs. 4(c) and 4(d), a 150-nm-thick VO_2 film deposited on sapphire exhibits "perfect" blackbody-like emissivity ~1 in the vicinity of the IMT (~74.5 °C) over a wavelength range of 40 cm^{-1}.[92]

Utilizing the distinct optical feature of VO_2 between metallic and insulating phases, several optical and radiative thermal devices have been proposed based on un-patterned thin films. A limiting optical diode, in which the phase transition of VO_2 is triggered asymmetrically depending on the direction of incident light [Figs. 4(h) and 4(i)], was designed using a stack comprising a semi-transparent metallic layer, a VO_2 layer, and a transparent substrate.[93] In such a device, a backward illumination triggers the IMT, hence resulting in a reduced transmission in that direction, while a forward illumination with the same intensity leaves the VO_2 state in its insulating phase, leading to high transmission. A similar yet different concept imagined exploiting VO_2 to control heat fluxes: a radiative thermal transistor, capable of modulating and amplifying radiative heat transfer in the far-field, was proposed by Joulain *et al.* [Figs. 4(j) and 4(k)].[94] By placing VO_2 between two blackbodies having different temperatures, a radiative flux amplification factor α larger than 1 can be achieved in the transition region from 341 K to 345 K driven by the emissivity variations of VO_2 at metallic and dielectric phases.

Engineering the geometric structure or spatial variation of phase through controlling the growth condition and introducing defects is another interesting method to fabricate metasurfaces without relying on etching processes. Using ion irradiation through masks [Figs. 4(l) and 4(m)], Rensberg *et al.* introduced defects into designated regions of VO_2 and locally changed the transition temperature.[95,96] As a result, a metasurface composed of metallic and insulating phases of VO_2 forms upon heating (T ~ 60 °C) and vanishes at temperatures away from it (e.g., 30 °C and 80 °C), the reflectance of which then shows engineered switchability and polarization dependence across the transition region between 25 °C and 90 °C. Another original method of creating "natural" metasurfaces can be obtained by controlling the structure and texture of VO_2 through specific strain governed by the substrate nature and orientation, as shown in Figs. 4(o) and 4(p). By using an a-cut $(11\bar{2}0)$ sapphire substrate that supports anisotropy growth, Ligmajer *et al.* grew a layer of self-structured VO_2 nanobeams having widths in the range of 100 nm–200 nm and lengths of 1000 nm–2000 nm.[97] The measured extinction spectra exhibited a broadband strong polarization dependence in both metallic and insulating phases. Such devices may be used for large-scale modulators with polarization control.

Given the large modifications in the local dielectric environment during the IMT, VO_2 can also be utilized as a tunable substrate to form heterostructures via direct contact with other photonic materials. Folland *et al.* reported a tunable hyperbolic metasurface device [Fig. 4(q)] by transferring a natural hyperbolic material medium—an isotopically enriched hexagonal boron nitride (*h*BN)—on top of a VO_2 crystal.[98] In their study, they demonstrated that the insulating and metallic domains of VO_2 can reflect, transmit, and launch hyperbolic phonon polaritons (HPhPs) at domain boundaries and showed a reconfigurable control of in-plane HPhP propagation. Modulation of the wavelength of HPhPs by a factor of 1.6 was achieved across these domains.

B. Dynamic modulation of spontaneous light emission

Since the pioneering work of Purcell, we know that the physics of spontaneous light emission is governed both by the quantum mechanical electronic transitions of the emitter and by the optical environment, also known as Local Density of Optical States (LDOS). As VO_2 presents very large modulations of its complex permittivity upon the IMT, it can be exploited to dynamically modify the LDOS and therefore open up interesting means to control the spontaneous emission of quantum emitters in integrated devices. This has been experimentally demonstrated in a multilayer stack comprising thin films of quantum emitters (Er^{3+}:Y_2O_3) and VO_2 [see Fig. 5(a)].[99] The device, comprising a quarter-wavelength phase-change layer located between an emitter layer and a metal mirror, was specifically designed such that the VO_2 IMT can be externally switched optically while also having optimized influence on the LDOS of the emitter layer. Upon switching the VO_2 layer, there is a π phase shift in the effective optical path length, which maximizes the influence

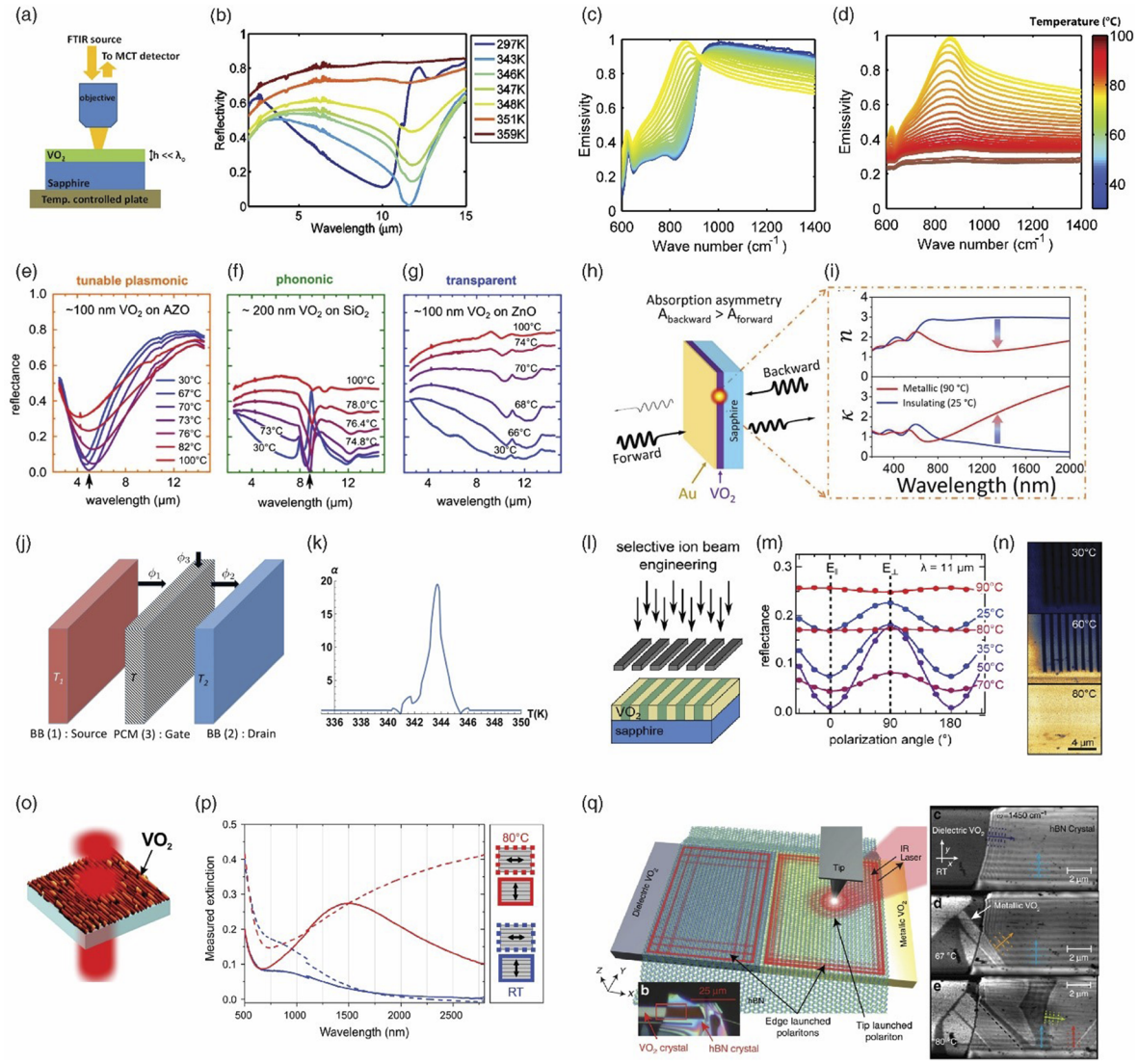

FIG. 4. Tunable metasurfaces using unpatterned VO_2 thin films. [(a) and (b)] Perfect absorber based on VO_2.[89] (a) Experimental setup for measuring the reflectivity of 180 nm VO_2 grown on a sapphire substrate. Reproduced with permission from M. A. Kats *et al.*, Appl. Phys. Lett. **101**, 221101 (2012).[89] Copyright 2012 AIP Publishing. (b) Temperature dependent reflectivity spectrum of devices where the reflectivity at 343 K approaches zero at $\lambda = 11.6\ \mu$m. [(c) and (d)] Perfect thermal emission of 150 nm VO_2 deposited on a sapphire substrate observed during heating from 35 °C to 74.5 °C (c) and from 74.5 °C–100 °C (d).[92] [(e)–(g)] Substrate engineering of VO_2-based thin film absorbers showing temperature dependent mid-IR reflectance of VO_2 on AZO (e), on SiO_2 (f), and on ZnO (g). Reprinted with permission from J. Rensberg *et al.*, Phys. Rev. Appl. **8**, 014009 (2017).[91] Copyright 2017 American Physical Society. [(h) and (i)] Limiting optical diode made from VO_2, where the intense backward illumination triggers the onset of the metallic phase, leading to reduced transmission, while VO_2 remains insulating when illuminating from the forward direction, resulting in high transmission. Adapted with permission from C. Wan *et al.*, ACS Photonics **5**, 2688–2692 (2018).[93] Copyright 2018 American Chemical Society. [(j) and (k)] Radiative thermal transistor based on metal–insulator transition of VO_2.[94] The transistor geometry is shown in (j) where a phase changing material, e.g., VO_2, is placed between two blackbodies. In the transition regime of VO_2, the amplification factor α of such a thermal transistor is larger than 1 (k). Reproduced with permission from K. Joulain *et al.*, Appl. Phys. Lett. **106**, 133505 (2015).[94] Copyright 2015 AIP Publishing. [(l)–(n)] Active metasurface built on defect engineered VO_2.[95] (l) Ion beam irradiation through a mask creates a defective region with a lower transition temperature. The pattern created by the pristine and irradiated VO_2 during heating (n) gives rise to a tunable polarization-dependent reflectance at $\lambda = 11\ \mu$m (m). Adapted with permission from J. Rensberg *et al.*, Nano Lett. **16**, 1050–1055 (2016).[95] Copyright 2016 American Chemical Society. [(o) and (p)] Tunable metasurface based on nanostructured VO_2 thin films.[97] (o) Metasurface with VO_2 nanobeams grown epitaxially on an a-cut sapphire substrate. (p) The extinction spectra of such a device at room temperature and 80 °C with incident light polarized perpendicular or parallel to the nanobeams, where the broad extinction peak at 1480 nm in the metallic state with perpendicular light is attributed to a localized surface plasmon resonance. Adapted with permission from F. Ligmajer *et al.*, ACS Photonics **5**, 2561–2567 (2018).[97] Copyright 2018 American Chemical Society. (q) Tunable infrared hyperbolic metasurface using VO_2, where hBN is transferred onto a VO_2 film and polaritons are imaged by an s-SNOM.[98] The change in the local dielectric environment from metallic to dielectric domains in VO_2 enables reconfigurable control of in-plane hyperbolic phonon polariton propagation.

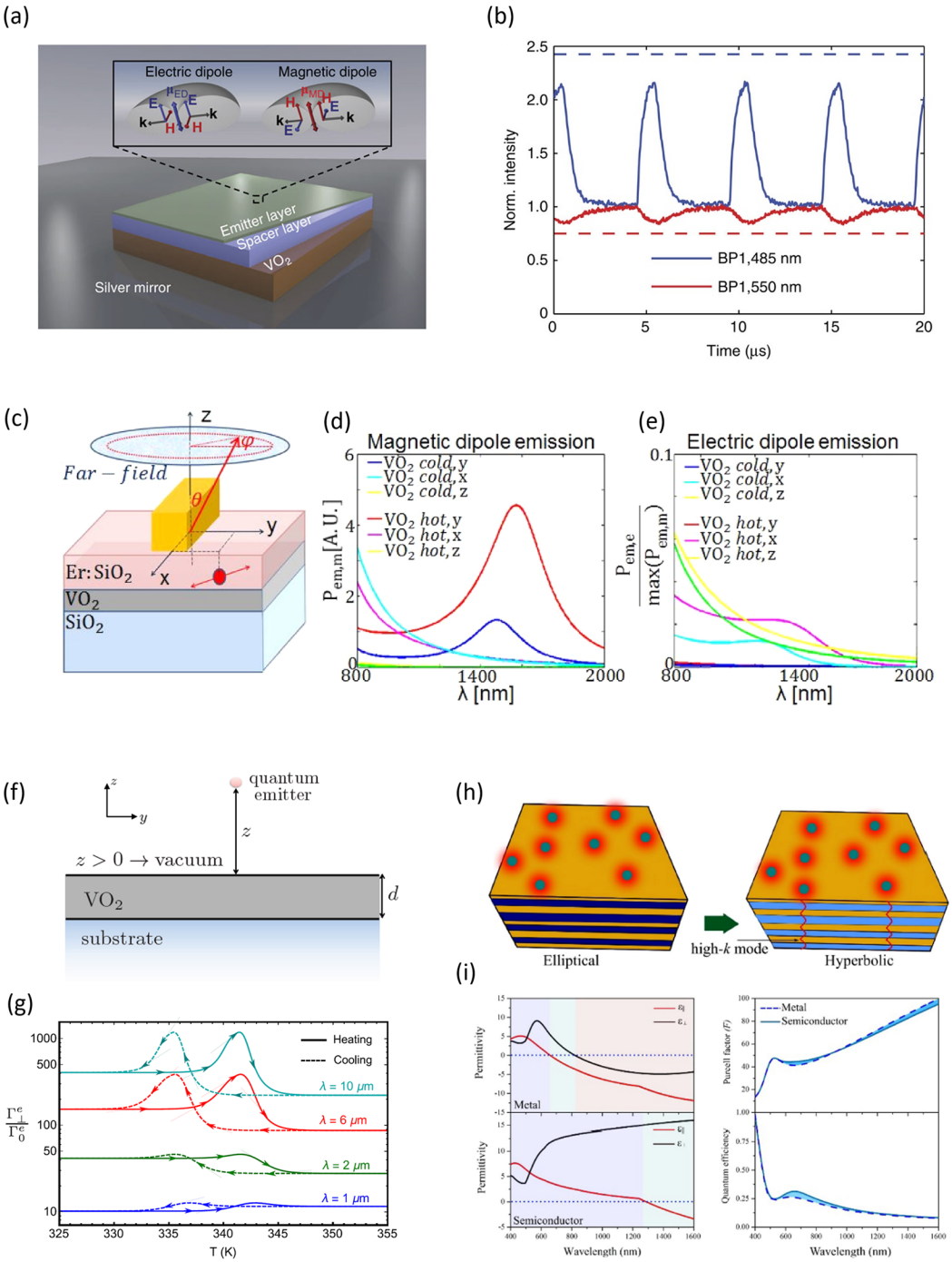

FIG. 5. Various methods and architectures for dynamically tuning the spontaneous emission of quantum emitters using VO_2 thin films. (a) A multilayer stack comprising a metallic mirror, a VO_2 layer, and an erbium thin film emitter[99] enables an all-optical direct modulation of spontaneous emission. (b) This modulation was experimentally demonstrated to be more than three orders of magnitude faster than the excited state lifetime of the erbium emitters. [(c)–(e)] A similar multilayer platform with an additional plasmonic antenna on top to further enhance the spontaneous emission rates [adapted with permission from E. Petronijevic *et al.*, Opt. Express **27**, 24260–24273 (2019).[101] Copyright 2019 The Optical Society]. [(f) and (g)] Enhancement of the ED and MD emission rates of quantum emitters in the vicinity of a VO_2 thin film during the IMT [adapted with permission from D. Szilard *et al.*, J. Opt. Soc. Am. B **36**, C46–C51 (2019).[127] Copyright 2019 The Optical Society]. [(h) and (i)] A multilayer stack whose optical dispersion is modulated from elliptical to hyperbolic via the change of phase of VO_2. The spontaneous emission rate of emitters is calculated to be affected by this dispersion modification [adapted with permission from S. K. Chamoli *et al.*, Opt. Lett. **45**, 1671–1674 (2020).[102] Copyright 2020 The Optical Society].

of the change in refractive index on the surrounding LDOS. Using this device, combined with the symmetry difference in the polarization of electric dipole (ED) and magnetic dipole (MD) transitions of erbium ions, one can dynamically switch between spectrally distinct ED-dominant and MD-dominant emission by simply changing the state of VO_2. With this concept, a broadband all-optical direct modulation of 1.5 μm emission from erbium ions was shown. Interestingly, such a dynamic optical modulation scheme was experimentally demonstrated to be more than three orders of magnitude faster than the excited state lifetime of the erbium emitters [see Fig. 5(b)], hence enabling fast direct modulation even for long lifetime quantum emitters.[99]

Other interesting ideas were further developed from that concept, as described in the following. Very recently, Jha *et al.* have used a similar configuration, in which VO_2 thin films are integrated in proximity to quantum emitters (*h*BN) as a means to modulate their LDOS. This tunable LDOS is then used to modulate the emission rate of quantum emitters, which, in turn, enabled resolving both the spatial position of the quantum emitter and its three-dimensional dipole orientation.[100] Szilard *et al.* have calculated the enhancement of the spontaneous rate of ED and MD emitters in the vicinity of VO_2 layers [see Figs. 5(f) and 5(g)].[127] They have shown that both ED and MD transition rates can be strongly enhanced, especially in the mid-infrared range at some specific stages of the IMT (in between insulator and metal). They further suggest that the IMT hysteresis could be used as another degree of freedom for dynamic control of the spontaneous emission with a memory effect. Other works studied the potential of VO_2 nanolayers associated with plasmonic antennas [see Figs. 5(c)–5(e)[101]] or hyperbolic metamaterials [Figs. 5(h) and 5(i)[102]] for further controlling the enhancement of spontaneous emission of quantum emitters.

C. Actively reconfigurable plasmonic antennas

In the last decade, VO_2 has been largely used as a means to control the resonance of plasmonic scatterers. These devices are usually based on plasmonic resonances in metallic nanostructures, fabricated on top of a VO_2 thin film.[13,41,89,103,104,128] Some of the earlier works were based on split-ring resonator devices patterned above VO_2 thin films.[13,105] By changing the phase of VO_2, the authors were able to controllably modify the resonant wavelength of the system in the MIR and visible range. Many different shapes and sizes of metallic nano-antennas were reported and experimentally demonstrated to be tuned by the underlying VO_2 thin film, spanning all wavelength regions from the visible to the terahertz range [see some selected examples in Figs. 6(a)–6(h)].

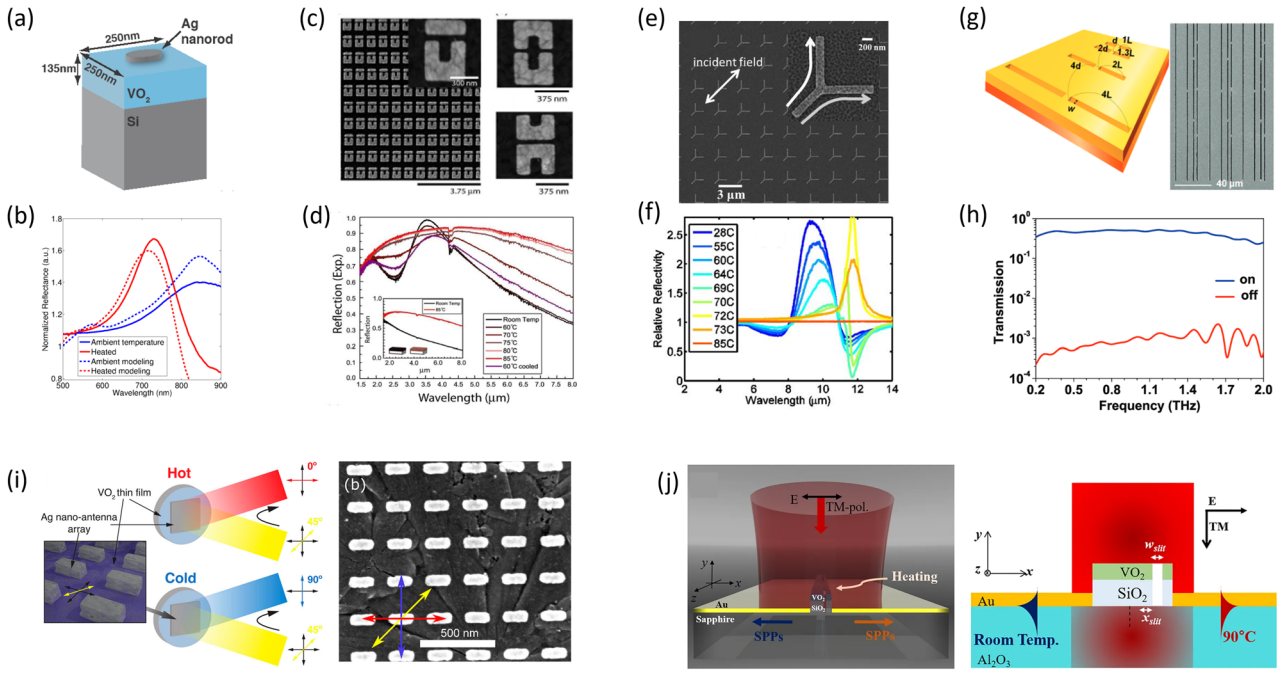

FIG. 6. Selected examples of tunable plasmonic antennas using VO_2. [(a)–(h)] Different architectures and geometries of metallic antennas on top of VO_2. The four selected examples have the same functionalities: dynamic modulation of transmission/reflection through the IMT of VO_2. By appropriately designing antennas, different spectral regions can be targeted from visible to terahertz ranges: [(a) and (b)] visible range using silver nanorods [adapted with permission from S. K. Earl *et al.*, Opt. Express **21**, 27503–27508 (2013).[103] Copyright 2013 The Optical Society]; [(c) and (d)] NIR with split-ring resonators [adapted with permission from M. J. Dicken *et al.*, Opt. Express **17**, 18330–18339 (2009).[13] Copyright 2009 The Optical Society]; [(e) and (f)] MIR with Y-shaped antennas [adapted with permission from M. A. Kats *et al.*, Opt. Lett. **38**, 368–370 (2013).[128] Copyright 2013 The Optical Society]; and [(g) and (h)] terahertz with gold slot antenna arrays [adapted with permission from M. Seo *et al.*, Nano Lett. **10**, 2064–2068 (2010).[104] Copyright 2010 American Chemical Society]. Other functionalities were demonstrated such as (i) switchable polarization rotation [reproduced with permission from S. K. Earl *et al.*, APL Photonics **2**, 016103 (2017).[110] Copyright 2017 AIP Publishing] or (j) active directional switching of surface plasmon polaritons.[111]

For the vast majority of these works, the VO_2 layer produces an amplitude modulation of the free-space reflection or transmission through the devices. Later on, numerous studies made use of similar plasmonic nano-element (disk, antenna, and slot) arrays for alternative applications such as optically triggered memory devices,[106] tunable color generation,[107,108] optical phase-arrays,[109] switchable polarization rotation,[110] and active directional switching of surface plasmon polaritons.[111] As VO_2 transitions from an insulator to a metal, Butakov *et al.* exploited this IMT to demonstrate switchable dielectric–plasmonic resonators using directly patterned VO_2 scatterers.[112] Alternatively, Muskens *et al.* exploited the spatially confined hotspots of antennas to locally switch VO_2 thin films. This method helped both reducing the energy consumption and the recovery time of VO_2, hence enabling reversible switching at over two million cycles per second, i.e., much faster than for a VO_2 thin film alone.[113]

VI. SUMMARY AND FUTURE PROMISING PERSPECTIVES

We have seen that VO_2 thin films have been used for about a decade to dynamically tune and switch nanophotonic devices, both for integrated guided wave optics and for free-space optics. In the majority of cases, VO_2 was used as a simple on–off optical switch, driven thermally or optically. Given its natural functionalities, we feel that this material is so far underused and its salient features such as the electrical control, the large hysteresis, and the multilevel intermediate states deserve to be better exploited in nanophotonic devices. We review in this section different works that explore these directions that we find particularly promising.

A. Electrically controlled tunable VO_2-based metasurfaces

As described previously, the IMT of VO_2 can be triggered via a large number of different stimuli. Among them, the electrical control of the state of VO_2 appears as the most useful implementation toward real world applications. Indeed, although it is much easier to demonstrate proof-of-concepts in a laboratory using controlled hot plates or lasers, many of the future applications should not rely on such external means of switching. Electrical control, on the other hand, is a widespread technique that is ubiquitous in modern devices. It is however challenging to create functional electrically controlled VO_2 devices for different reasons. The first one is mainly technological: it is not straightforward to integrate electrodes with VO_2, or even to nanopattern it altogether, because this material combines a high-reactivity with most of the wet-etchant chemicals used to process metals and a good resistance to a common dry-etching process. This implies that the technological processes for this platform are not yet mature and require internal developments for each laboratory. The second and most important reason is that a design that would work for thermal or optical switching has little chance to be readily adapted for electrical excitation. This is due to the presence of electrodes that obviously introduce differences in the overall optical properties. The architectures of devices should therefore be completely redesigned to properly take into account the influence of electrodes. This should not be seen as a limitation of the technology but rather as another layer of complexity that has to be thought through. In this section, we therefore review interesting advances in experimental demonstrations of electrically controlled VO_2-based devices for nanophotonics.

One of the first works on the electrical control of VO_2 to tune an integrated optical device was reported by Driscoll *et al.* in 2009.[12] In this study, the authors demonstrated a frequency-agile metamaterial based on split-ring resonators operating in the THz range [see Fig. 7(a)]. Using a simple planar electrode architecture at controlled temperatures, they were able to electrically induce persistent tuning of the metamaterial's resonance. Following this pioneering demonstration, a few works reported the electrical control of the VO_2 state on top of silicon-based waveguides, as described in Sec. IV.[68,69] More recently, three different groups reported experimental demonstrations of electrically controlled VO_2-based nanophotonic devices. Liu *et al.* proposed, in 2016,[114] a metal–insulator–metal configuration, comprising a VO_2 thin film sandwiched in between metal antennas and a dielectric spacer, as displayed in Figs. 7(d) and 7(e). Interestingly, the top metallic cross-shaped antennas are patterned as an array that connects them together, hence enabling electrical current to flow through the structure and to electrically trigger the IMT of VO_2. The authors then demonstrated a very large optical reflectance modulation from ~0% to ~80% at a wavelength of 3 μm upon electrically switching VO_2. This report was followed a year later (2017) by the experimental demonstration of a near-infrared spectral tuning of metadevices comprising VO_2 nano-elements placed at the feed gap of bow-tie antenna suspended membranes.[115] As shown in Fig. 7(b), VO_2 unit cells, about ~30 nm-wide, are all electrically connected via metallic lines and the spectral tuning is driven by Joule heating. This configuration presents the advantage of minimizing the volume of VO_2, hence reducing thermal mass, energy consumption, and switching times (reported to be in the millisecond range). These two demonstrations were followed in 2019 by the report of an electrically triggered modulation of optical phase in a one-dimensional metasurface array of metal–VO_2–insulator–metal waveguides [see Figs. 7(f) and 7(g)].[116] In this study, the electrical control follows the same principle as in the two previous works: the patterned metallic structures on top of VO_2 serve as a means to distribute the flowing current throughout the device and trigger the VO_2 IMT via Joule heating. Using this reflectarray architecture, the authors report a phase modulation as high as 250°, accompanied by spectral tuning and intensity modulation. This is the first demonstration of electrically tunable continuous optical phase modulation using VO_2.

This "trilogy" of reports therefore nicely demonstrates that VO_2-based devices enable the active modulation of the intensity, spectrum, and phase of reflected fields via electrical means. These works therefore pave the way for future efficient electrical control of different aspects of light fields for free-space optics using metasurface-inspired configurations. Future works in that field may focus on improving metrics such as the optical efficiency and the switching time that are so far relatively modest. Designing devices that can separately modulate the amplitude and phase of the reflected/transmitted optical fields via electrical control appear to be very challenging but if successful would unlock such technologies for multifunctional integrated tunable devices.

B. Tackling the absorption issue

The non-negligible optical absorption in both states of VO_2 could be a major drawback for most applications as a tunable

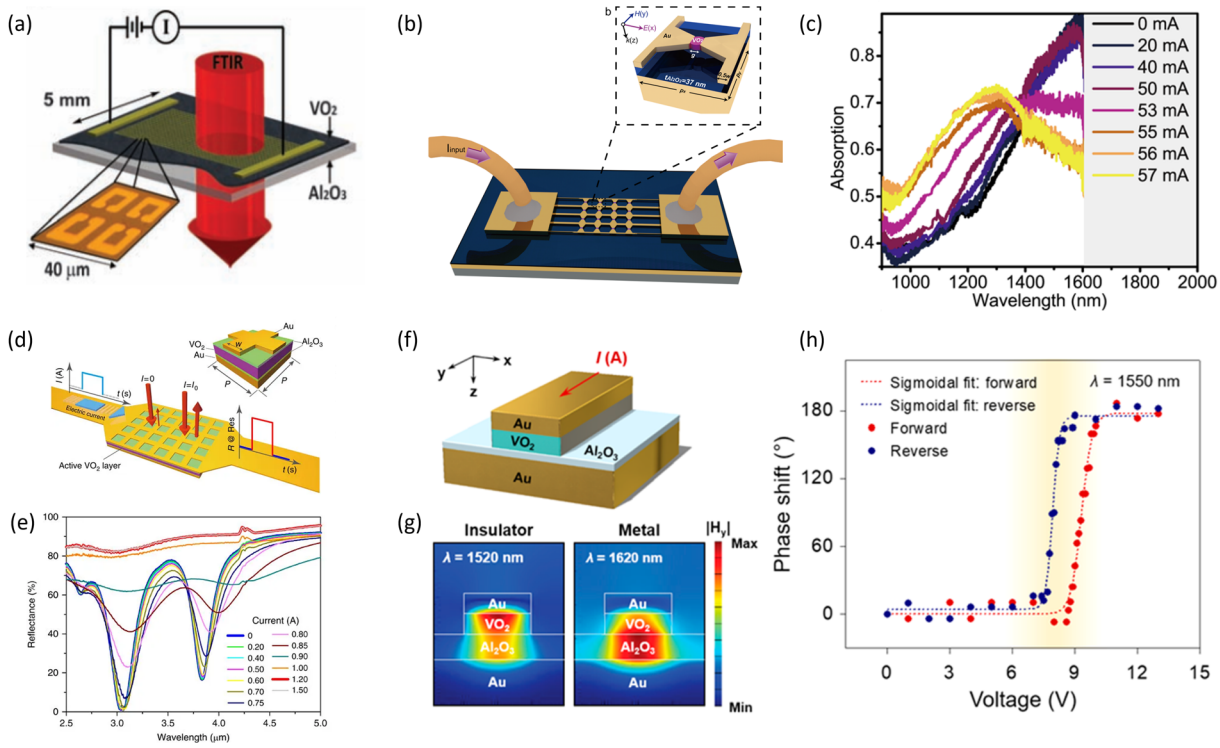

FIG. 7. Electrically controlled optical modulation using VO_2. (a) Tunable transmission in the terahertz domain using an array of split-ring resonators. Reproduced with permission from T. Driscoll *et al.*, Science **325**, 1518–1521 (2009).[12] Copyright 2009 AAAS. [(b) and (c)] Array of electrically connected hybrid metal/VO_2 antennas. Adapted with permission from Z. Zhu *et al.*, Nano Lett. **17**, 4881–4885 (2017).[115] Copyright 2017 American Chemical Society. The electrical switching of VO_2 nano-elements enables tuning of the optical absorption in the NIR. [(d) and (e)] A metal–insulator–VO_2–metal stack comprising a connected array of antennas.[114] The electrical switching of VO_2 produces a large modulation of the transmission through the progressive disappearance of the plasmonic resonances. [(f)–(h)] A similar metal–insulator–VO_2–metal stack arranged in a one-dimensional photonic crystal array. Adapted with permission from Y. Kim *et al.*, Nano Lett. 19, 3961–3968 (2019).[116] Copyright 2019 American Chemical Society. The electrically induced IMT switch here produces a π phase-shift, hence enabling a tunable phase modulation metasurface.

optical medium. We review here two main strategies to mitigate this issue.

One straightforward solution is to design devices in spectral regions where the absorption is the lowest. As shown in Fig. 1(g), the extinction coefficient of VO_2 in its insulating state slowly decreases at longer wavelengths and reaches a minimum down to k ~0.07 in the range 2 μm–10 μm. When excited to the metallic state, the extinction coefficient dramatically increases, up to values of k ~ 5–10. In that range of the mid-IR, there is therefore room to design devices with low losses in one state and large absorption in the other state. This combination of features would be particularly useful for compact on–off modulators with large extinction ratios, both for guided and free-space optics. Looking back at the previously described results, we can indeed observe that the devices showing the highest modulation amplitudes are those designed for this wavelength range [see, e.g., Figs. 4(a), 4(b), and 7(e)] in which reflection modulation from ~0% to ~80% were demonstrated at wavelengths of 11 μm and 3 μm, respectively. This wavelength region appears also very promising for integrated guided wave optics, as many recent works demonstrated low-loss mid-IR waveguides on various platforms such as silicon, germanium, or SiGe.[117] We foresee that the use of VO_2 for mid-IR guided optics should lead to very interesting devices and large-scale tunable systems in the near future.

Another solution to avoid the large losses in VO_2 is to appropriately engineer the hybrid photonic structure of VO_2. One way of doing so is to use ultra-thin films of VO_2. Indeed, the complex refractive index modulation of VO_2 is so large that a few nanometers of material suffices for active tuning in many devices. As previously mentioned, VO_2 is a complex material whose growing conditions are far from being straightforward. Fabricating ultra-thin films of VO_2 is therefore challenging in itself. Quackenbush *et al.* reported the successful growth of ultra-thin films (7.5 nm–1 nm) of VO_2 by molecular beam epitaxy.[118,119] Interestingly, they demonstrated that the IMT of VO_2 remains unchanged even for 1-nm-thick layers (i.e., about two unit cells). This important result holds promise for the future use of ultra-thin functional layers of VO_2. Recently, Guo *et al.* reported the use of atomic layer deposition (ALD) to grow ultrathin layers of VO_2.[120] With this method, they demonstrated the conformal coating of VO_2 layers on ITO nanorod arrays [see Figs. 8(a) and 8(b)]. Such a growing technique appears promising to seamlessly implement ultrathin layers of VO_2 on nanostructures with an overall low optical absorption.

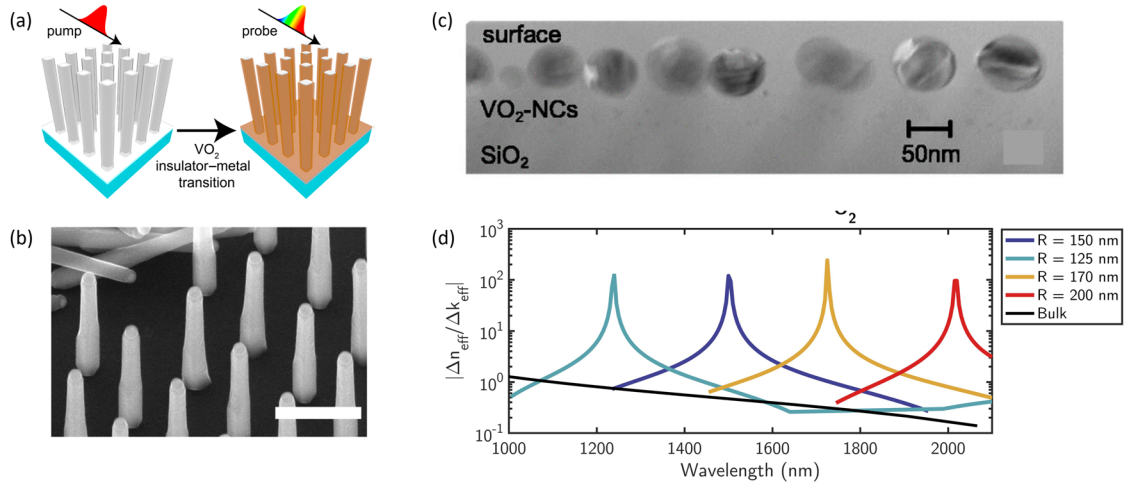

FIG. 8. Different methods of mitigating the optical absorption of VO_2 by reducing its size: [(a) and (b)] ALD method enables growing ultra-thin and conformal layers of VO_2 [adapted with permission from P. Guo *et al.*, ACS Nano **11**, 693–701 (2017).[120] Copyright 2017 American Chemical Society] and [(c) and (d)] VO_2-nanocrystals help reducing the overall optical absorption and increase the figure of merit $\Delta n/\Delta k$ [reprinted with permission from J. John *et al.* Phys. Rev. Appl. **13**, 044053 (2020).[121] Copyright 2020 by the American Physical Society].

It was recently shown that VO_2 nanocrystals (VO_2-NCs) implanted in SiO_2 as spherical nanoinclusions [see Fig. 8(c)] provide an alternative path toward low-loss tunable media.[121] By exploiting the VO_2 IMT, it is possible to tune and switch multipolar modes supported by VO_2-NCs in the visible and to gradually produce a plasmonic mode in the NIR whose intensity is directly controlled by the VO_2 state. It was shown that the complex refractive index of such an effective medium (a slab of VO_2 nanospheres embedded in SiO_2) presents distinct optical tunability compared to unpatterned VO_2. By adjusting the VO_2-NC size, the effective medium can be designed to have a large refractive-index tunability without inducing modulation of the extinction coefficient at specific wavelengths. This zero-induced-extinction refractive index tuning opens up new regimes of record large figure of merit ($\Delta n/\Delta k$) and designer optical tunability, unattainable with conventional unpatterned PCM layers [see Fig. 8(c)], and suggests a new practical direction to produce low-loss tunable optical metamaterials.

C. Spatially addressed optical control of IMT and memory effects

As mentioned in Sec. III, VO_2 is known to present a broad hysteresis in its IMT cycle. This hysteresis can be, to some extent, engineered via strain or doping.[14,15,35,122] However, there is a surprisingly low number of papers that actually use this functionality in devices. Such an effect can be used to demonstrate memory effects. Lei *et al.* exploited this hysteresis to demonstrate an all-optical memory effect in hybrid plasmonic nanostructures.[106] More recently, Fan *et al.* reported an optoelectronic memory device with electrical writing and optical reading using epitaxial VO_2 thin films grown on GaN.[123] The memory effect has also been demonstrated in hybrid VO_2/Si waveguides.[63] Such memory devices are still volatile in nature though, as their "memory" state only lasts several microseconds at best. However, we describe in the following three recent works that elegantly exploited the hysteretic behavior of VO_2 to demonstrate all-optical non-volatile nanophotonic devices.

The VO_2-NCs described in Sec. VI B typically present an ultra-broad hysteresis behavior, with an IMT occurring at ~80 °C upon heating and a relaxation to the insulating state at ~25 °C upon cooling [see Fig. 9(a)]. Hence, by keeping the sample at temperatures as low as ~30 °C, it is possible to maintain a persistent metallic state in VO_2-NCs. Jostmeier *et al.* exploited that functionality to optically imprint photonic elements onto an unpatterned VO_2-NC platform.[124] Using a visible laser scanned at specific points of the sample, they locally switch VO_2-NCs and define patterns such as gratings and zone plates, as shown in Fig. 9(a). This original technique appears as a very flexible way to fabricate reconfigurable photonic devices as they can later be erased by simply cooling down the sample to room temperature.

Two recent works used the same principle to optically imprint arbitrary reconfigurable patterns via locally switching the state of VO_2 thin films. The first one, reported in 2018 by Dong *et al.*,[125] demonstrated the dynamic writing and erasing of arbitrary patterns and reconfigurable photonic devices such as beam-steerers, linear polarizers, and concentric-ring gratings at a wavelength of 10.6 μm [see Fig. 9(b)]. Each of the patterns, fabricated using a 532 nm laser, can be "stored" in the VO_2 film by maintaining the sample at temperatures around the IMT, i.e., ~60 °C. They coined this reconfigurable VO_2-based platform a "programmable metacanvas." A following recent work used the same method to demonstrate a spatially resolved control of thermal emission in a large wavelength range of the mid-IR (8 μm–14 μm).[126] As shown in Fig. 9(c), they exploited both the hysteresis and the intermediate phases of VO_2 to write non-volatile multilevel states in the thin layer, each producing a different level of thermal emission.

These three works demonstrate very promising ways to fully exploit VO_2 for its hysteretic behavior and large optical modulation in the mid-IR. One may find the need for temperature control to be

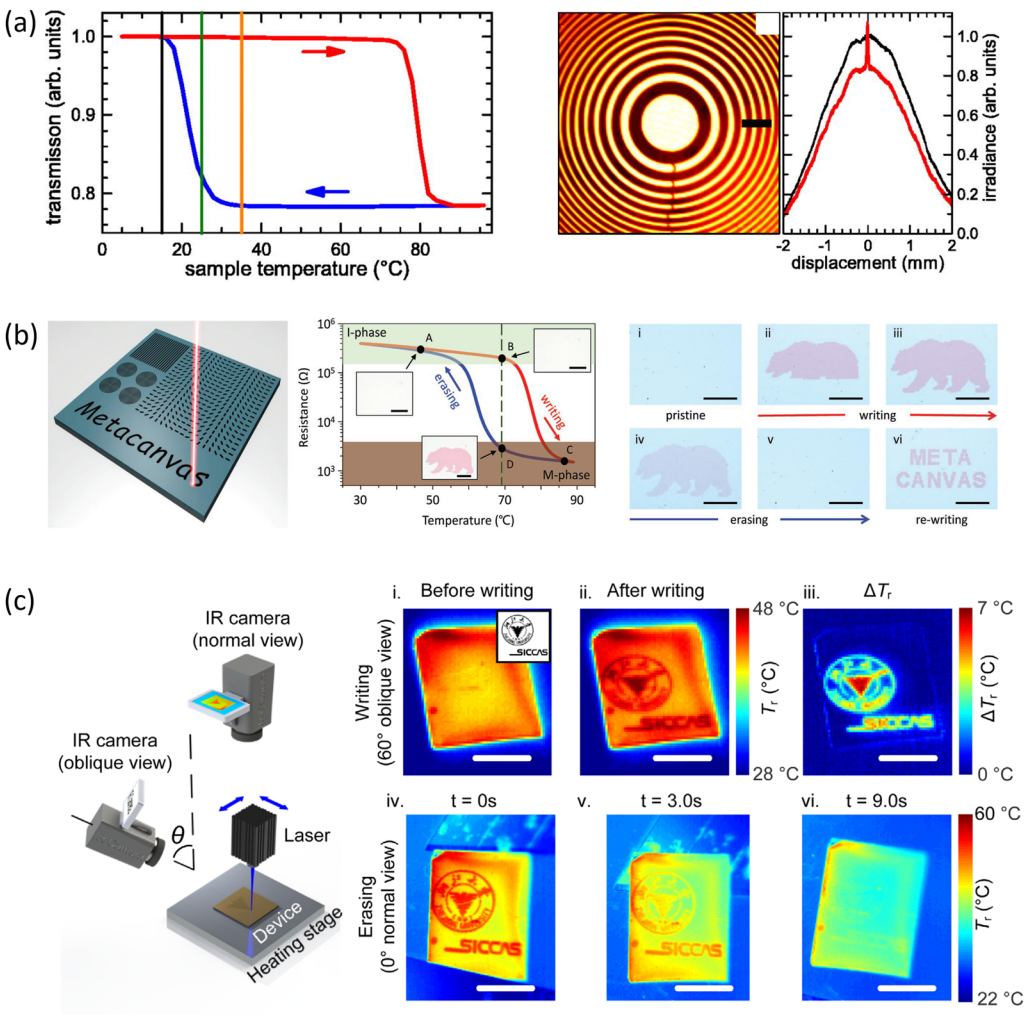

FIG. 9. Examples of spatially addressed tunable regions and VO_2-based optically imprinted optical elements with memory effects. (a) The laser imprinting of optical devices was demonstrated on the VO_2-NC platform, and the large hysteresis behavior, typical in these VO_2-NCs, enables storing such structures as non-volatile devices by maintaining the samples at temperatures close to RT (~30 °C). Reproduced with permission from T. Jostmeier *et al.*, Appl. Phys. Lett. **105**, 071107 (2014).[124] Copyright 2014 AIP Publishing. (b) The so-called "programmable metacanvas" utilizing both the hysteresis and the local optical switching of VO_2 to fabricate and erase reconfigurable photonic devices. Adapted with permission from K. Dong *et al.*, Adv. Mater. **30**, 1703878 (2018).[125] Copyright 2018 Wiley-VCH. (c) A similar concept of a locally controlled VO_2 state using laser-scanning techniques to fabricate devices. In addition, the authors demonstrated the optical writing of multilevel states and controlled thermal emission.[126]

inconvenient, but this could alternatively be seen as a very practical method to easily erase and reconfigure devices. These demonstrations may pave the way for future real-time adaptive optical systems.

D. Ultra-fast switching time in integrated devices

Finally, a very important open question remains on whether ultra-fast switching times, below the picosecond range, are actually feasible in practical hybrid integrated devices. All-optical switching seems to be the most promising approach based on previous experiments on non-integrated devices (see, for instance, Ref. 39). However, ultra-fast all-optical switching on hybrid integrated devices has only been very recently demonstrated.[81] The key point is to control and minimize the thermal component associated with the VO_2 phase transition without penalizing the optical switching performance.

All in all, progress toward a better use and integration of VO_2 in nanophotonic devices will go in parallel with progress in better understanding and control of the complex physics of VO_2.

ACKNOWLEDGMENTS

S.C. acknowledges funding from the French National Research Agency (ANR) under the project SNAPSHOT (Grant No. ANR-16-CE24-0004). Z.Z. and S.R. acknowledge AFOSR (Grant No. FA9550-18-1-0250) for support. P.S. acknowledges Generalitat Valenciana

(No. PROMETEO/2019/123), Ministerio de Economía y Competitividad (MINECO/FEDER, UE) (No. TEC2016-76849) and Ministerio de Ciencia e Innovacion (MINECO/FEDER, UE) (No. PID2019-111460GB-I00). J.P. acknowledges the Ministerio de Ciencia, Innovación y Universidades for his grant (Grant No. FPU17/04224). We thank M. Kats for fruitful discussions and feedback on the manuscript.

DATA AVAILABILITY

Data sharing is not applicable to this article as no new data were created or analyzed in this study.

REFERENCES

[1] L. Novotny and B. Hecht, *Principles of Nano-Optics* (Cambridge University Press, 2012).
[2] A. F. Koenderink, A. Alu, and A. Polman, "Nanophotonics: Shrinking light-based technology," Science **348**, 516–521 (2015).
[3] J. W. Haus, *Fundamentals and Applications of Nanophotonics* (Woodhead Publishing, 2016).
[4] N. Yu and F. Capasso, "Flat optics with designer metasurfaces," Nat. Mater. **13**, 139–150 (2014).
[5] S. M. Kamali, E. Arbabi, A. Arbabi, and A. Faraon, "A review of dielectric optical metasurfaces for wavefront control," Nanophotonics **7**, 1041–1068 (2018).
[6] Z. Yang, C. Ko, and S. Ramanathan, "Oxide electronics utilizing ultrafast metal-insulator transitions," Annu. Rev. Mater. Res. **41**, 337–367 (2011).
[7] S. Raoux, "Phase change materials," Annu. Rev. Mater. Res. **39**, 25–48 (2009).
[8] F. J. Morin, "Oxides which show a metal-to-insulator transition at the Neel temperature," Phys. Rev. Lett. **3**, 34 (1959).
[9] A. S. Barker, Jr., H. W. Verleur, and H. J. Guggenheim, "Infrared optical properties of vanadium dioxide above and below the transition temperature," Phys. Rev. Lett. **17**, 1286 (1966).
[10] H. W. Verleur, A. S. Barker, Jr., and C. N. Berglund, "Optical properties of VO_2 between 0.25 and 5 eV," Phys. Rev. **172**, 788 (1968).
[11] T. Driscoll, S. Palit, M. M. Qazilbash, M. Brehm, F. Keilmann, B.-G. Chae, S.-J. Yun, H.-T. Kim, S. Y. Cho, N. M. Jokerst *et al.*, "Dynamic tuning of an infrared hybrid-metamaterial resonance using vanadium dioxide," Appl. Phys. Lett. **93**, 024101 (2008).
[12] T. Driscoll, H.-T. Kim, B.-G. Chae, B.-J. Kim, Y.-W. Lee, N. M. Jokerst, S. Palit, D. R. Smith, M. Di Ventra, and D. N. Basov, "Memory metamaterials," Science **325**, 1518–1521 (2009).
[13] M. J. Dicken, K. Aydin, I. M. Pryce, L. A. Sweatlock, E. M. Boyd, S. Walavalkar, J. Ma, and H. A. Atwater, "Frequency tunable near-infrared metamaterials based on VO_2 phase transition," Opt. Express **17**, 18330–18339 (2009).
[14] K. Liu, S. Lee, S. Yang, O. Delaire, and J. Wu, "Recent progresses on physics and applications of vanadium dioxide," Mater. Today **21**, 875–896 (2018).
[15] R. Shi, N. Shen, J. Wang, W. Wang, A. Amini, N. Wang, and C. Cheng, "Recent advances in fabrication strategies, phase transition modulation, and advanced applications of vanadium dioxide," Appl. Phys. Rev. **6**, 011312 (2019).
[16] Y. Ke, S. Wang, G. Liu, M. Li, T. J. White, and Y. Long, "Vanadium dioxide: The multistimuli responsive material and its applications," Small **14**, 1802025 (2018).
[17] N. Mott, *Metal-Insulator Transitions* (CRC Press, 2004).
[18] M. Imada, A. Fujimori, and Y. Tokura, "Metal-insulator transitions," Rev. Mod. Phys. **70**, 1039 (1998).
[19] J. H. Park, J. M. Coy, T. S. Kasirga, C. Huang, Z. Fei, S. Hunter, and D. H. Cobden, "Measurement of a solid-state triple point at the metal–insulator transition in VO_2," Nature **500**, 431–434 (2013).
[20] J. P. Pouget and H. Launois, "Metal-insulator phase transition in VO_2," J. Phys. Colloq. **37**, C4–C49 (1976).
[21] M. Marezio, D. B. McWhan, J. P. Remeika, and P. D. Dernier, "Structural aspects of the metal-insulator transitions in Cr-doped VO_2," Phys. Rev. B **5**, 2541 (1972).
[22] M. Ghedira, H. Vincent, M. Marezio, and J. C. Launay, "Structural aspects of the metal-insulator transitions in $V_{0.985}AL_{0.015}O_2$," J. Solid State Chem. **22**, 423–438 (1977).
[23] R. E. Peierls, *Quantum Theory of Solids* (Clarendon Press, 1996).
[24] T. Huffman, C. Hendriks, E. Walter, J. Yoon, H. Ju, R. Smith, G. Carr, H. Krakauer, and M. Qazilbash, "Insulating phases of vanadium dioxide are Mott-Hubbard insulators," Phys. Rev. B **95**, 075125 (2017).
[25] V. Eyert, "The metal-insulator transitions of VO_2: A band theoretical approach," Ann. Phys. **11**, 650–704 (2002).
[26] V. Eyert, "VO_2: A novel view from band theory," Phys. Rev. Lett. **107**, 016401 (2011).
[27] S. Biermann, A. Poteryaev, A. Lichtenstein, and A. Georges, "Dynamical singlets and correlation-assisted Peierls transition in VO_2," Phys. Rev. Lett. **94**, 026404 (2005).
[28] Z. He and A. J. Millis, "Photoinduced phase transitions in narrow-gap Mott insulators: The case of VO_2," Phys. Rev. B **93**, 115126 (2016).
[29] M. van Veenendaal, "Ultrafast photoinduced insulator-to-metal transitions in vanadium dioxide," Phys. Rev. B **87**, 235118 (2013).
[30] F. Grandi, A. Amaricci, and M. Fabrizio, "Unraveling the Mott-Peierls intrigue in vanadium dioxide," Phys. Rev. Res. **2**, 013298 (2020).
[31] V. R. Morrison, R. P. Chatelain, K. L. Tiwari, A. Hendaoui, A. Bruhács, M. Chaker, and B. J. Siwick, "A photoinduced metal-like phase of monoclinic VO_2 revealed by ultrafast electron diffraction," Science **346**, 445–448 (2014).
[32] R. Yoshida, T. Yamamoto, Y. Ishida, H. Nagao, T. Otsuka, K. Saeki, Y. Muraoka, R. Eguchi, K. Ishizaka, T. Kiss *et al.*, "Ultrafast photoinduced transition of an insulating VO_2 thin film into a nonrutile metallic state," Phys. Rev. B **89**, 205114 (2014).
[33] T. Cocker, L. Titova, S. Fourmaux, G. Holloway, H.-C. Bandulet, D. Brassard, J.-C. Kieffer, M. El Khakani, and F. Hegmann, "Phase diagram of the ultrafast photoinduced insulator-metal transition in vanadium dioxide," Phys. Rev. B **85**, 155120 (2012).
[34] Z. Tao, T.-R. T. Han, S. D. Mahanti, P. M. Duxbury, F. Yuan, C.-Y. Ruan, K. Wang, and J. Wu, "Decoupling of structural and electronic phase transitions in VO_2," Phys. Rev. Lett. **109**, 166406 (2012).
[35] J. Laverock, S. Kittiwatanakul, A. Zakharov, Y. Niu, B. Chen, S. Wolf, J. Lu, and K. Smith, "Direct observation of decoupled structural and electronic transitions and an ambient pressure monoclinic like metallic phase of VO_2," Phys. Rev. Lett. **113**, 216402 (2014).
[36] C. Ko and S. Ramanathan, "Observation of electric field-assisted phase transition in thin film vanadium oxide in a metal-oxide-semiconductor device geometry," Appl. Phys. Lett. **93**, 252101 (2008).
[37] Y. Zhou, X. Chen, C. Ko, Z. Yang, C. Mouli, and S. Ramanathan, "Voltage-triggered ultrafast phase transition in vanadium dioxide switches," IEEE Electron Device Lett. **34**, 220–222 (2013).
[38] G. Stefanovich, A. Pergament, and D. Stefanovich, "Electrical switching and Mott transition in VO_2," J. Phys.: Condens. Matter **12**, 8837 (2000).
[39] A. Cavalleri, C. Tóth, C. W. Siders, J. Squier, F. Ráksi, P. Forget, and J. Kieffer, "Femtosecond structural dynamics in VO_2 during an ultrafast solid-solid phase transition," Phys. Rev. Lett. **87**, 237401 (2001).
[40] A. Cavalleri, T. Dekorsy, H. H. Chong, J.-C. Kieffer, and R. W. Schoenlein, "Evidence for a structurally-driven insulator-to-metal transition in VO_2: A view from the ultrafast timescale," Phys. Rev. B **70**, 161102 (2004).
[41] M. Liu, H. Y. Hwang, H. Tao, A. C. Strikwerda, K. Fan, G. R. Keiser, A. J. Sternbach, K. G. West, S. Kittiwatanakul, J. Lu *et al.*, "Terahertz-field-induced insulator-to-metal transition in vanadium dioxide metamaterial," Nature **487**, 345–348 (2012).
[42] H. Kakiuchida, P. Jin, S. Nakao, and M. Tazawa, "Optical properties of vanadium dioxide film during semiconductive–metallic phase transition," Jpn. J. Appl. Phys., Part 2 **46**, L113 (2007).
[43] J. Sun and G. K. Pribil, "Analyzing optical properties of thin vanadium oxide films through semiconductor-to-metal phase transition using spectroscopic ellipsometry," Appl. Surf. Sci. **421**, 819–823 (2017).
[44] C. Wan, Z. Zhang, D. Woolf, C. M. Hessel, J. Rensberg, J. M. Hensley, Y. Xiao, A. Shahsafi, J. Salman, S. Richter *et al.*, "On the optical properties of thin-film

vanadium dioxide from the visible to the far infrared," Ann. Phys. **531**, 1900188 (2019).
[45]S. Amador-Alvarado, J. Flores-Camacho, A. Solís-Zamudio, R. Castro-García, J. Pérez-Huerta, E. Antúnez-Cerón, J. Ortega-Gallegos, J. Madrigal-Melchor, V. Agarwal, and D. Ariza-Flores, "Temperature-dependent infrared ellipsometry of Mo-doped VO_2 thin films across the insulator to metal transition," Sci. Rep. **10**, 8555 (2020).
[46]J. T. Swann and D. J. De Smet, "Ellipsometric investigation of vanadium dioxide films," J. Appl. Phys. **58**, 1335–1338 (1985).
[47]M. A. Motyka, B. D. Gauntt, M. W. Horn, E. C. Dickey, and N. J. Podraza, "Microstructural evolution of thin film vanadium oxide prepared by pulsed-direct current magnetron sputtering," J. Appl. Phys. **112**, 093504 (2012).
[48]M. M. Qazilbash, M. Brehm, B.-G. Chae, P.-C. Ho, G. O. Andreev, B.-J. Kim, S. J. Yun, A. V. Balatsky, M. B. Maple, F. Keilmann *et al.*, "Mott transition in VO_2 revealed by infrared spectroscopy and nano-imaging," Science **318**, 1750–1753 (2007).
[49]A. Perucchi, L. Baldassarre, P. Postorino, and S. Lupi, "Optical properties across the insulator to metal transitions in vanadium oxide compounds," J. Phys.: Condens. Matter **21**, 323202 (2009).
[50]J. Wei, H. Ji, W. Guo, A. H. Nevidomskyy, and D. Natelson, "Hydrogen stabilization of metallic vanadium dioxide in single-crystal nanobeams," Nat. Nanotechnol. **7**, 357–362 (2012).
[51]H. Yoon, M. Choi, T.-W. Lim, H. Kwon, K. Ihm, J. K. Kim, S.-Y. Choi, and J. Son, "Reversible phase modulation and hydrogen storage in multivalent VO_2 epitaxial thin films," Nat. Mater. **15**, 1113–1119 (2016).
[52]S. A. Dönges, O. Khatib, B. T. O'Callahan, J. M. Atkin, J. H. Park, D. Cobden, and M. B. Raschke, "Ultrafast nanoimaging of the photoinduced phase transition dynamics in VO_2," Nano Lett. **16**, 3029–3035 (2016).
[53]S. Zhang, J. Y. Chou, and L. J. Lauhon, "Direct correlation of structural domain formation with the metal insulator transition in a VO_2 nanobeam," Nano Lett. **9**, 4527–4532 (2009).
[54]R. M. Briggs, I. M. Pryce, and H. A. Atwater, "Compact silicon photonic waveguide modulator based on the vanadium dioxide metal-insulator phase transition," Opt. Express **18**, 11192–11201 (2010).
[55]J. D. Ryckman, K. A. Hallman, R. E. Marvel, R. F. Haglund, and S. M. Weiss, "Ultra-compact silicon photonic devices reconfigured by an optically induced semiconductor-to-metal transition," Opt. Express **21**, 10753–10763 (2013).
[56]G. T. Reed, G. Mashanovich, F. Y. Gardes, and D. J. Thomson, "Silicon optical modulators," Nat. Photonics **4**, 518–526 (2010).
[57]K. Yao, R. Unni, and Y. Zheng, "Intelligent nanophotonics: Merging photonics and artificial intelligence at the nanoscale," Nanophotonics **8**, 339–366 (2019).
[58]J. Wang, F. Sciarrino, A. Laing, and M. G. Thompson, "Integrated photonic quantum technologies," Nat. Photonics **14**, 273 (2019).
[59]K. Liu, C. R. Ye, S. Khan, and V. J. Sorger, "Review and perspective on ultrafast wavelength-size electro-optic modulators," Laser Photonics Rev. **9**, 172–194 (2015).
[60]K. Shibuya, Y. Atsumi, T. Yoshida, Y. Sakakibara, M. Mori, and A. Sawa, "Silicon waveguide optical modulator driven by metal–insulator transition of vanadium dioxide cladding layer," Opt. Express **27**, 4147–4156 (2019).
[61]L. Sanchez, S. Lechago, A. Gutierrez, and P. Sanchis, "Analysis and design optimization of a hybrid VO_2/silicon 2 × 2 microring switch," IEEE Photonics J. **8**, 1–9 (2016).
[62]K. J. Miller, K. A. Hallman, R. F. Haglund, and S. M. Weiss, "Silicon waveguide optical switch with embedded phase change material," Opt. Express **25**, 26527–26536 (2017).
[63]I. Olivares, L. Sánchez, J. Parra, R. Larrea, A. Griol, M. Menghini, P. Homm, L.-W. Jang, B. van Bilzen, J. W. Seo *et al.*, "Optical switching in hybrid VO_2/Si waveguides thermally triggered by lateral microheaters," Opt. Express **26**, 12387–12395 (2018).
[64]L. D. Sánchez, I. Olivares, J. Parra, M. Menghini, P. Homm, J.-P. Locquet, and P. Sanchis, "Experimental demonstration of a tunable transverse electric pass polarizer based on hybrid VO_2/silicon technology," Opt. Lett. **43**, 3650–3653 (2018).
[65]B. Janjan, M. Miri, D. Fathi, M. Heidari, and D. Abbott, "Hybrid Si_3N_4/VO_2 modulator thermally triggered by a graphene microheater," IEEE J. Sel. Top. Quantum Electron. **26**, 1 (2020).
[66]V. Jeyaselvan, A. Pal, P. S. Anil Kumar, and S. K. Selvaraja, "Thermally-induced optical modulation in a vanadium dioxide-on-silicon waveguide," OSA Continuum **3**, 132–142 (2020).
[67]M. Sadeghi, B. Janjan, M. Heidari, and D. Abbott, "Mid-infrared hybrid Si/VO_2 modulator electrically driven by graphene electrodes," Opt. Express **28**, 9198–9207 (2020).
[68]P. Markov, R. E. Marvel, H. J. Conley, K. J. Miller, R. F. Haglund, Jr., and S. M. Weiss, "Optically monitored electrical switching in VO_2," ACS Photonics **2**, 1175–1182 (2015).
[69]A. Joushaghani, J. Jeong, S. Paradis, D. Alain, J. S. Aitchison, and J. K. S. Poon, "Wavelength-size hybrid Si-VO_2 waveguide electroabsorption optical switches and photodetectors," Opt. Express **23**, 3657–3668 (2015).
[70]J. T. Kim, "CMOS-compatible hybrid plasmonic modulator based on vanadium dioxide insulator-metal phase transition," Opt. Lett. **39**, 3997–4000 (2014).
[71]P. Markov, K. Appavoo, R. F. Haglund, and S. M. Weiss, "Hybrid Si-VO_2-Au optical modulator based on near-field plasmonic coupling," Opt. Express **23**, 6878–6887 (2015).
[72]J.-H. Choe and J. T. Kim, "Design of vanadium dioxide-based plasmonic modulator for both TE and TM modes," IEEE Photonics Technol. Lett. **27**, 514–517 (2014).
[73]S. Mohammadi-Pouyan, M. Miri, and M. H. Sheikhi, "Design of a vanadium dioxide-based dual-polarization optical PAM4 modulator," J. Opt. Soc. Am. B **35**, 3094–3103 (2018).
[74]B. M. Younis, A. M. Heikal, M. Hussein, S. S. A. Obayya, and M. F. O. Hameed, "Hybrid Si-VO_2 modulator with ultra-high extinction ratio based on slot TM mode," Opt. Express **27**, 37454–37468 (2019).
[75]L. Sánchez, A. Rosa, A. Griol, A. Gutierrez, P. Homm, B. Van Bilzen, M. Menghini, J. P. Locquet, and P. Sanchis, "Impact of the external resistance on the switching power consumption in VO_2 nano gap junctions," Appl. Phys. Lett. **111**, 031904 (2017).
[76]J. D. Ryckman, V. Diez-Blanco, J. Nag, R. E. Marvel, B. K. Choi, R. F. Haglund, and S. M. Weiss, "Photothermal optical modulation of ultra-compact hybrid Si-VO_2 ring resonators," Opt. Express **20**, 13215–13225 (2012).
[77]L. Chen, H. Ye, Y. Liu, D. Wu, R. Ma, and Z. Yu, "Numerical investigations of an optical switch based on a silicon stripe waveguide embedded with vanadium dioxide layers," Photonics Res. **5**, 335–339 (2017).
[78]J. K. Clark, Y.-L. Ho, H. Matsui, and J.-J. Delaunay, "Optically pumped hybrid plasmonic-photonic waveguide modulator using the VO_2 metal-insulator phase transition," IEEE Photonics J. **10**, 1–9 (2017).
[79]R. F. Haglund, K. A. Hallman, K. J. Miller, and S. M. Weiss, "Picosecond optical switching in silicon photonics using phase-changing vanadium dioxide," in *CLEO: Science and Innovations* (Optical Society of America, 2019), STh4H-1.
[80]H. M. K. Wong, Z. Yan, K. A. Hallman, R. E. Marvel, R. P. Prasankumar, R. F. Haglund, Jr., and A. S. Helmy, "Broadband, integrated, micron-scale, all-optical Si_3N_4/VO_2 modulators with pJ switching energy," ACS Photonics **6**, 2734–2740 (2019).
[81]K. A. Hallman, K. J. Miller, A. Baydin, S. M. Weiss, and R. F. Haglund, "Sub-picosecond all-optical switching in a hybrid VO_2:silicon waveguide at 1550 nm," arXiv:2007.02812 (2020).
[82]J. Parra, T. Ivanova, M. Menghini, P. Homm, J.-P. Locquet, and P. Sanchis, "Temporal dynamics of all-optical switching in hybrid VO_2/Si waveguides," arXiv:2007.11452 (2020).
[83]D. Wegkamp, M. Herzog, L. Xian, M. Gatti, P. Cudazzo, C. L. McGahan, R. E. Marvel, R. F. Haglund, Jr., A. Rubio, M. Wolf *et al.*, "Instantaneous band gap collapse in photoexcited monoclinic VO_2 due to photocarrier doping," Phys. Rev. Lett. **113**, 216401 (2014).
[84]Z. Tao, F. Zhou, T.-R. T. Han, D. Torres, T. Wang, N. Sepulveda, K. Chang, M. Young, R. R. Lunt, and C.-Y. Ruan, "The nature of photoinduced phase transition and metastable states in vanadium dioxide," Sci. Rep. **6**, 38514 (2016).
[85]M. R. Otto, L. P. R. de Cotret, D. A. Valverde-Chavez, K. L. Tiwari, N. Émond, M. Chaker, D. G. Cooke, and B. J. Siwick, "How optical excitation controls the

structure and properties of vanadium dioxide," Proc. Natl. Acad. Sci. U. S. A. **116**, 450–455 (2019).
[86]S. Wang, P. C. Wu, V.-C. Su, Y.-C. Lai, M.-K. Chen, H. Y. Kuo, B. H. Chen, Y. H. Chen, T.-T. Huang, J.-H. Wang *et al.*, "A broadband achromatic metalens in the visible," Nat. Nanotechnol. **13**, 227–232 (2018).
[87]A. Arbabi, E. Arbabi, Y. Horie, S. M. Kamali, and A. Faraon, "Planar metasurface retroreflector," Nat. Photonics **11**, 415 (2017).
[88]G. Zheng, H. Mühlenbernd, M. Kenney, G. Li, T. Zentgraf, and S. Zhang, "Metasurface holograms reaching 80% efficiency," Nat. Nanotechnol. **10**, 308–312 (2015).
[89]M. A. Kats, D. Sharma, J. Lin, P. Genevet, R. Blanchard, Z. Yang, M. M. Qazilbash, D. N. Basov, S. Ramanathan, and F. Capasso, "Ultra-thin perfect absorber employing a tunable phase change material," Appl. Phys. Lett. **101**, 221101 (2012).
[90]N. A. Butakov, M. W. Knight, T. Lewi, P. P. Iyer, D. Higgs, H. T. Chorsi, J. Trastoy, J. Del Valle Granda, I. Valmianski, C. Urban *et al.*, "Broadband electrically tunable dielectric resonators using metal–insulator transitions," ACS Photonics **5**, 4056–4060 (2018).
[91]J. Rensberg, Y. Zhou, S. Richter, C. Wan, S. Zhang, P. Schöppe, R. Schmidt-Grund, S. Ramanathan, F. Capasso, M. A. Kats *et al.*, "Epsilon-near-zero substrate engineering for ultrathin-film perfect absorbers," Phys. Rev. Appl. **8**, 014009 (2017).
[92]M. A. Kats, R. Blanchard, S. Zhang, P. Genevet, C. Ko, S. Ramanathan, and F. Capasso, "Vanadium dioxide as a natural disordered metamaterial: Perfect thermal emission and large broadband negative differential thermal emittance," Phys. Rev. X **3**, 041004 (2013).
[93]C. Wan, E. H. Horak, J. King, J. Salman, Z. Zhang, Y. Zhou, P. Roney, B. Gundlach, S. Ramanathan, R. H. Goldsmith *et al.*, "Limiting optical diodes enabled by the phase transition of vanadium dioxide," ACS Photonics **5**, 2688–2692 (2018).
[94]K. Joulain, Y. Ezzahri, J. Drevillon, and P. Ben-Abdallah, "Modulation and amplification of radiative far field heat transfer: Towards a simple radiative thermal transistor," Appl. Phys. Lett. **106**, 133505 (2015).
[95]J. Rensberg, S. Zhang, Y. Zhou, A. S. McLeod, C. Schwarz, M. Goldflam, M. Liu, J. Kerbusch, R. Nawrodt, S. Ramanathan *et al.*, "Active optical metasurfaces based on defect-engineered phase-transition materials," Nano Lett. **16**, 1050–1055 (2016).
[96]Z. Zhang, F. Zuo, C. Wan, A. Dutta, J. Kim, J. Rensberg, R. Nawrodt, H. H. Park, T. J. Larrabee, X. Guan *et al.*, "Evolution of metallicity in vanadium dioxide by creation of oxygen vacancies," Phys. Rev. Appl. **7**, 034008 (2017).
[97]F. Ligmajer, L. Kejík, U. Tiwari, M. Qiu, J. Nag, M. Konečný, T. Šikola, W. Jin, R. F. Haglund, Jr., K. Appavoo *et al.*, "Epitaxial VO_2 nanostructures: A route to large-scale, switchable dielectric metasurfaces," ACS Photonics **5**, 2561–2567 (2018).
[98]T. G. Folland, A. Fali, S. T. White, J. R. Matson, S. Liu, N. A. Aghamiri, J. H. Edgar, R. F. Haglund, Y. Abate, and J. D. Caldwell, "Reconfigurable infrared hyperbolic metasurfaces using phase change materials," Nat. Commun. **9**, 4371 (2018).
[99]S. Cueff, D. Li, Y. Zhou, F. J. Wong, J. A. Kurvits, S. Ramanathan, and R. Zia, "Dynamic control of light emission faster than the lifetime limit using VO_2 phase-change," Nat. Commun. **6**, 8636 (2015).
[100]P. K. Jha, H. Akbari, Y. Kim, and H. A. Atwater, "Nanoscale axial position and orientation measurement of hexagonal boron nitride quantum emitters using a tunable nanophotonic environment," arXiv:2007.07811 (2020).
[101]E. Petronijevic, M. Centini, T. Cesca, G. Mattei, F. A. Bovino, and C. Sibilia, "Control of Au nanoantenna emission enhancement of magnetic dipolar emitters by means of VO_2 phase change layers," Opt. Express **27**, 24260–24273 (2019).
[102]S. K. Chamoli, M. ElKabbash, J. Zhang, and C. Guo, "Dynamic control of spontaneous emission rate using tunable hyperbolic metamaterials," Opt. Lett. **45**, 1671–1674 (2020).
[103]S. K. Earl, T. D. James, T. J. Davis, J. C. McCallum, R. E. Marvel, R. F. Haglund, and A. Roberts, "Tunable optical antennas enabled by the phase transition in vanadium dioxide," Opt. Express **21**, 27503–27508 (2013).
[104]M. Seo, J. Kyoung, H. Park, S. Koo, H.-s. Kim, H. Bernien, B. J. Kim, J. H. Choe, Y. H. Ahn, H.-T. Kim *et al.*, "Active terahertz nanoantennas based on VO_2 phase transition," Nano Lett. **10**, 2064–2068 (2010).
[105]K. Appavoo and R. F. Haglund, Jr., "Detecting nanoscale size dependence in VO_2 phase transition using a split-ring resonator metamaterial," Nano Lett. **11**, 1025–1031 (2011).
[106]D. Y. Lei, K. Appavoo, F. Ligmajer, Y. Sonnefraud, R. F. Haglund, Jr., and S. A. Maier, "Optically-triggered nanoscale memory effect in a hybrid plasmonic-phase changing nanostructure," ACS Photonics **2**, 1306–1313 (2015).
[107]S. Song, X. Ma, M. Pu, X. Li, Y. Guo, P. Gao, and X. Luo, "Tailoring active color rendering and multiband photodetection in a vanadium-dioxide-based metamaterial absorber," Photonics Res. **6**, 492–497 (2018).
[108]F.-Z. Shu, F.-F. Yu, R.-W. Peng, Y.-Y. Zhu, B. Xiong, R.-H. Fan, Z.-H. Wang, Y. Liu, and M. Wang, "Dynamic plasmonic color generation based on phase transition of vanadium dioxide," Adv. Opt. Mater. **6**, 1700939 (2018).
[109]G. Kaplan, K. Aydin, and J. Scheuer, "Dynamically controlled plasmonic nano-antenna phased array utilizing vanadium dioxide," Opt. Mater. Express **5**, 2513–2524 (2015).
[110]S. K. Earl, T. D. James, D. E. Gómez, R. E. Marvel, R. F. Haglund, Jr., and A. Roberts, "Switchable polarization rotation of visible light using a plasmonic metasurface," APL Photonics **2**, 016103 (2017).
[111]S.-J. Kim, H. Yun, K. Park, J. Hong, J.-G. Yun, K. Lee, J. Kim, S. J. Jeong, S.-E. Mun, J. Sung *et al.*, "Active directional switching of surface plasmon polaritons using a phase transition material," Sci. Rep. **7**, 43723 (2017).
[112]N. A. Butakov, I. Valmianski, T. Lewi, C. Urban, Z. Ren, A. A. Mikhailovsky, S. D. Wilson, I. K. Schuller, and J. A. Schuller, "Switchable plasmonic–dielectric resonators with metal–insulator transitions," ACS Photonics **5**, 371–377 (2018).
[113]O. L. Muskens, L. Bergamini, Y. Wang, J. M. Gaskell, N. Zabala, C. De Groot, D. W. Sheel, and J. Aizpurua, "Antenna-assisted picosecond control of nanoscale phase transition in vanadium dioxide," Light: Sci. Appl. **5**, e16173 (2016).
[114]L. Liu, L. Kang, T. S. Mayer, and D. H. Werner, "Hybrid metamaterials for electrically triggered multifunctional control," Nat. Commun. **7**, 13236 (2016).
[115]Z. Zhu, P. G. Evans, R. F. Haglund, Jr., and J. G. Valentine, "Dynamically reconfigurable metadevice employing nanostructured phase-change materials," Nano Lett. **17**, 4881–4885 (2017).
[116]Y. Kim, P. C. Wu, R. Sokhoyan, K. Mauser, R. Glaudell, G. Kafaie Shirmanesh, and H. A. Atwater, "Phase modulation with electrically tunable vanadium dioxide phase-change metasurfaces," Nano Lett. **19**, 3961–3968 (2019).
[117]R. Soref, "Mid-infrared photonics in silicon and germanium," Nat. Photonics **4**, 495–497 (2010).
[118]N. F. Quackenbush, J. W. Tashman, J. A. Mundy, S. Sallis, H. Paik, R. Misra, J. A. Moyer, J.-H. Guo, D. A. Fischer, J. C. Woicik *et al.*, "Nature of the metal insulator transition in ultrathin epitaxial vanadium dioxide," Nano Lett. **13**, 4857–4861 (2013).
[119]N. F. Quackenbush, H. Paik, J. C. Woicik, D. A. Arena, D. G. Schlom, and L. F. Piper, "X-ray spectroscopy of ultra-thin oxide/oxide heteroepitaxial films: A case study of single-nanometer VO_2/TiO_2," Materials **8**, 5452–5466 (2015).
[120]P. Guo, M. S. Weimer, J. D. Emery, B. T. Diroll, X. Chen, A. S. Hock, R. P. H. Chang, A. B. F. Martinson, and R. D. Schaller, "Conformal coating of a phase change material on ordered plasmonic nanorod arrays for broadband all-optical switching," ACS Nano **11**, 693–701 (2017).
[121]J. John, Y. Gutierrez, Z. Zhang, H. Karl, S. Ramanathan, R. Orobtchouk, F. Moreno, and S. Cueff, "Multipolar resonances with designer tunability using VO_2 phase-change materials," Phys. Rev. Appl. **13**, 044053 (2020).
[122]X. Tan, T. Yao, R. Long, Z. Sun, Y. Feng, H. Cheng, X. Yuan, W. Zhang, Q. Liu, C. Wu *et al.*, "Unraveling metal-insulator transition mechanism of VO_2 triggered by tungsten doping," Sci. Rep. **2**, 466 (2012).
[123]L. Fan, Y. Chen, Q. Liu, S. Chen, L. Zhu, Q. Meng, B. Wang, Q. Zhang, H. Ren, and C. Zou, "Infrared response and optoelectronic memory device fabrication based on epitaxial VO_2 film," ACS Appl. Mater. Interfaces **8**, 32971–32977 (2016).
[124]T. Jostmeier, J. Zimmer, H. Karl, H. J. Krenner, and M. Betz, "Optically imprinted reconfigurable photonic elements in a VO_2 nanocomposite," Appl. Phys. Lett. **105**, 071107 (2014).

[125]K. Dong, S. Hong, Y. Deng, H. Ma, J. Li, X. Wang, J. Yeo, L. Wang, S. Lou, K. B. Tom *et al.*, "A lithography-free and field-programmable photonic metacanvas," Adv. Mater. **30**, 1703878 (2018).
[126]Z. Xu, Q. Li, K. Du, S. Long, Y. Yang, X. Cao, H. Luo, H. Zhu, P. Ghosh, W. Shen *et al.*, "Spatially resolved dynamically reconfigurable multilevel control of thermal emission," Laser Photonics Rev. **14**, 1900162 (2020).
[127]D. Szilard, W. J. M. Kort-Kamp, F. S. S. Rosa, F. A. Pinheiro, and C. Farina, "Hysteresis in the spontaneous emission induced by VO_2 phase change," J. Opt. Soc. Am. B **36**, C46–C51 (2019).
[128]M. A. Kats, R. Blanchard, P. Genevet, Z. Yang, M. M. Qazilbash, D. N. Basov, S. Ramanathan, and F. Capasso, "Thermal tuning of mid-infrared plasmonic antenna arrays using a phase change material," Opt. Lett. **38**, 368–370 (2013).